THOMSON REUTERS
ENDNOTE

[Bagoury*, 5(2): February, 2016]

ISSN: 2277-9655
(I2OR), Publication Impact Factor: 3.785

IJESRT

INTERNATIONAL JOURNAL OF ENGINEERING SCIENCES & RESEARCH TECHNOLOGY

NI BASED SUPERALLOY: CASTING TECHNOLOGY, METALLURGY, DEVELOPMENT, PROPERTIES AND APPLICATIONS

Nader El-Bagoury

Chemistry Department, Faculty of Science, TAIF University, P.O. Box 888, El-Haweyah, El-Taif, Saudi Arbia.
Central Metallurgical Research and Development Institute (CMRDI), P.O. Box 87, Helwan, Cairo, Egypt.

ABSTRACT

A superalloy, or high-performance alloy, is an alloy able to withstand extreme temperatures that would destroy conventional metals like steel and aluminum. Nickel based superalloys are selected for use in certain applications due to their characteristics. These alloys have an exceptional combination of high temperature strength, toughness, and resistance to degradation in corrosive or oxidizing environments. Among the important characteristics are creep resistance at high temperatures, good surface stability, and corrosion and oxidation resistance. Because of these characteristics they are widely used in aircraft and power-generation turbines, rocket engines, nuclear power and chemical processing plants and other challenging environments. The availability of superalloys during past decades has led to a steady increase in the turbine entry temperatures, and this trend is expected to continue. New generations of superalloys can tolerate average temperatures of 1050°C with occasional excursions to temperatures as high as 1200°C, which is approximately 90% of the melting point of the material. Increased operating temperatures and higher efficiency in gas turbines and jet engines can reduce CO_2 emission, thus contributing to the slowing of climate change.

KEYWORDS: Ni Base Superalloys, casting, metallurgy, development, properties, applications.

Nomenclature

Ni	Nickel
TIT	Turbine Inlet Temperature
Hastellloy X	Solid solution strengthened Ni base super alloy
γ	Matrix phase in Ni-base superalloy
γ′	Ni_3Al(Ti, Nb) precipitate phase in a Ni base superalloy with L12 structure
FCC	face centered cubic structure
L12	FCC superlattice of the Ni_3Al type
γ "	Ni_3Nb precipitate phase in Ni base superalloy
BCT	Body centered tetragonal
TCP	Topologically close-packed
GCP	geometrically close-packed
δ	Delta phase precipitated Ni base superalloys
μ	Myo phase precipitated Ni base superalloys
Laves	Ni_2Nb phase precipitated Ni base superalloys
σ	Sigma phase precipitated Ni base superalloys
VIM	Vacuum induction melting
ppm	part per million
VIDP	vacuum induction melting degassing and pouring
DS	Directionally solidified
SX	Single Crystal
HABs	high angle boundaries
SC	Single Crystal
CC	conventional casting
Re	Rhenium
Cr	Chromium
Co	Cobalt

Mo	Molybdenum
W	Tungsten
Al	Aluminum
Ti	Titanium
Ta	Tantalum
Nb	Niobium
V	Vanadium
Ru	Ruthenium
GE	General Electric
NIMS	National Institute of Materials Science
B	Boron
Zr	Zirconium
C	Carbon
Hf	Hafnium
V_f	volume fraction
Fe	Iron
Y	Yttrium
MA	mechanically alloyed
ODS	oxide dispersion-strengthened
PM	powder metallurgy
a_γ	lattice parameter for gamma phase
Å	angstrom equal 10^{-10} m
C_i	in atom-parts in the γ -mixed crystal
a and c	lattice parameters of a body centered tetragonal lattice
APB	anti-phase boundary
TBC	thermal barrier coating
IPC	intermediate pressure compressor
HPC	high pressure compressor
HPT	high pressure compressor turbine
IPT	intermediate pressure turbine
LPT	low pressure turbine
T_m	melting point temperature
MME	metal mold equilibrium
SDAS	secondary dendrite arm spacing
λ_2	secondary dendrite arm spacing
SLA	Stereo Lithography
LOM	Laminated Object Manufacturing
SGC	Solid Ground Curing
FDM	Fused Deposition Modeling
SLS	Selective Laser Sintering
DMLS	Direct Metal Laser Sintering
Ir	iridium
Rh	rhodium
ρ	density

INTRODUCTION

Superalloys or high-performance alloys are the materials able to withstand extreme temperatures that would destroy conventional metals like steel, titanium and aluminum. The term "superalloy" was first used shortly after World War II to describe a group of alloys developed for use in turbo-superchargers and aircraft turbine engines that required high performance at elevated temperatures. The range of applications for which superalloys are used has expanded too many other areas and now includes aircraft and land-based gas turbines, rocket engines, chemical, and petroleum plants. They are particularly well suited for these demanding applications because of their ability to retain most of their strength even

after long exposure times above 650°C. Their versatility stems from the fact that they combine this high strength with good low-temperature ductility and excellent surface stability **[1, 2].**

Ni base superalloys are multicomponent complex alloys which, in addition to Ni, contain varying amounts of Cr, Mo, W, Nb, Al, Ti, Ta, Re, Hf, Zr, B, and C to obtain the desired strength, oxidation resistance, and corrosion resistance. Superalloys have been under intense and continuing development since the early 1940's **[3-5].**

At 1950's, the evolution from wrought to conventionally cast, Table 1, to directionally solidified to single crystal turbine blades has yielded a 250°C increase in allowable metal temperatures, and cooling developments have nearly doubled this in terms of turbine entry gas temperature. An important recent contribution has come from the alignment of the alloy grain in the single crystal blade, which has allowed the elastic properties of the material to be controlled more closely. These properties in turn control the natural vibration frequencies of the blade **[6, 7].**

Nickel-based alloys can be either solid solution or precipitation strengthened. Solid solution strengthened alloys, such as Hastelloy X, are used in applications requiring only modest strength. In the most demanding applications, such as hot sections of gas turbine engines, a precipitation strengthened alloy is required. Most nickel-based alloys contain 10-20% Cr, up to 8% Al and Ti, 5-10% Co, and small amounts of B, Zr, and C. Other common additions are Mo, W, Ta, Hf, and Nb. In broad terms, the elemental additions in Ni-base superalloys can be categorized as being:

- γ formers (elements that tend to partition to the γ matrix).
- γ' formers (elements that partition to the γ ' precipitate).
- Carbide formers.
- Elements that segregate to the grain boundaries such as B, C, and Zr **[8-10].**

The widespread use of superalloys in turbine engines coupled with the fact that the thermodynamic efficiency of turbine engines is increased with increasing turbine inlet temperatures [1]. A superalloy is a metallic alloy which is developed to resist most of all high temperatures, usually in cases until 70 % of the absolute melting temperature. All of these alloys have an excellent creep, corrosion and oxidation resistance as well as a good surface stability and fatigue life.

The main alloying elements are nickel, cobalt or nickel – iron, which can be found in the 8^{th} group of the periodic system of the elements.
Fields of application are found particularly in the aerospace industry and in the nuclear industries, e.g. for engines and turbines.

The development of these advanced alloys allows a better exploitation of engines, which work at high temperatures, because the Turbine Inlet Temperature (TIT) depends on the temperature capability of the material which forms the turbine blades.

Ni based superalloys have an austenitic face-centered cubic, which delivers advantages such as:

- better mechanical properties
- higher modulus
- higher solubility of alloying elements
- systems of gliding plane

FUNDAMENTALS OF NICKEL-BASE SUPERALLOYS

Nickel-based superalloys can be strengthened through solid-solution and precipitation. The solid-solution strengthens superalloys, such as Hastelloy X, are used for burner and combustor applications in gas turbine engines. They have particularly high-temperature corrosion resistance, excellent fabricability and weldability but lower mechanical strength. The precipitation-strengthened alloys are constituted in applications requiring high-temperature strength and good corrosion and creep resistance, for instance as turbine blades and vanes in the gas turbine.

Nickel-based superalloys can be used for a higher fraction of melting temperature and are therefore more favourable than cobalt-based and iron-nickel-based superalloys at service temperatures close to the melting temperature of the materials **[11].**

CLASSIFICATION OF SUPERALLOYS

Superalloys are heat-resisting alloys based on nickel, nickel-iron, or cobalt that exhibit a combination of mechanical strength and resistance to surface degradation. Superalloys exhibit excellent mechanical strength and creep resistance at high temperatures, good surface stability, and corrosion and oxidation resistance. Superalloys typically have an austenitic face-centered cubic crystal structure. Superalloy development has relied heavily on both chemical and process innovations and has been driven primarily by the aerospace and power industries. Typical applications are in the aerospace industry, e.g. for turbine blades for jet engines **[12].**

MICROSTRUCTURE OF NI BASE SUPERALLOYS :

4.1. Gamma (γ) phase

The continuous matrix (called gamma), **Fig. 1**, is a face-centered-cubic (fcc) nickel-based austenitic phase. The continuous phase is nonmagnetic. Because nickel has a nearly filled 3rd electronic shell, which allows alloying with solid solution strengthening elements without losses in phase stability. The alloy elements assembling mainly the gamma matrix belong to Group V, VI and VII and are cobalt, iron, chromium, molybdenum and tungsten, **Fig. 2**. The atomic diameters of these alloys are only 3-13% different than Ni (the primary matrix element). These alloys contains a high percentage of solid solution elements as shown in **Fig. 3 (a).**

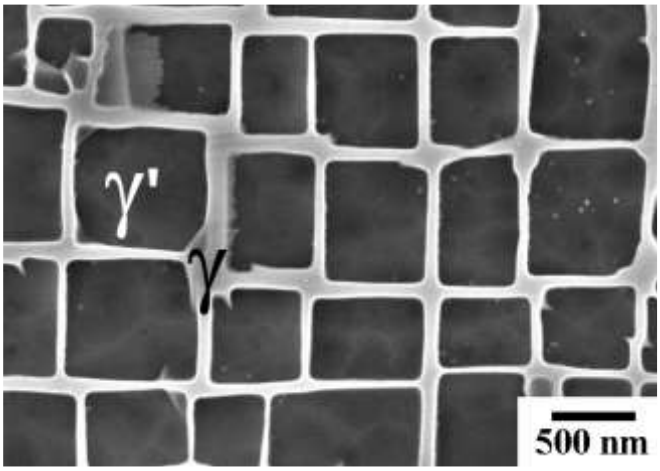

Fig. 1 γ′ precipitates as cubic morphology in γ matrix. [11]

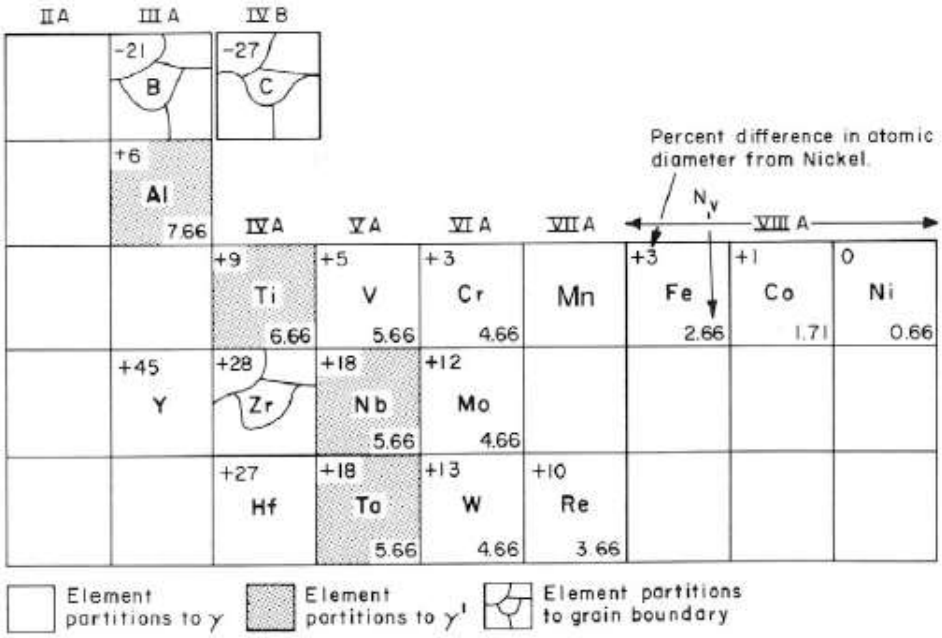

Figure 2 Main alloying and partioning elements.

Gamma Prime (γ') phase

The primary strengthening phase in nickel-based superalloys is $Ni_3(Al,Ti)$, and is called gamma prime (γ'). It is a coherently precipitating phase (i.e., the crystal planes of the precipitate are in registry with the gamma matrix) with an ordered $L1_2$ (FCC) crystal structure, **Fig. 3 (b)**. The close match in matrix/precipitate lattice parameter (~0-1%) combined with the chemical compatibility allows the γ' to precipitate homogeneously throughout the matrix and have long-time stability, **Fig. 1**. Interestingly, the yield stress of the γ' increases with increasing temperature up to about 650ºC (1200ºF). In addition, γ' is quite ductile and thus imparts strength to the matrix without lowering the fracture toughness of the alloy. Aluminum and titanium are the major constituents in γ', beside Ni, and are added in various amounts and mutual proportions to precipitate a high volume fraction of γ' in the matrix. The atomic diameters of these elements differ from Ni by 16-18%. In some modern alloys the volume fraction of the γ' precipitate is about 70%. There are many factors that contribute to the hardening imparted by the γ' and include γ' fault energy, γ' strength, coherency strains, volume fraction of γ', and γ' particle size **[13, 14]**.

In contrast the interfacial energy can be minimized by forming cubes. Thus as the □′ grows, the morphology can change from spheres to cubes or plates depending on the value of the matrix/precipitate lattice mismatch. If the mismatch is larger, the critical particle size reduces where the change takes place. Coherency can be lost by overageing.

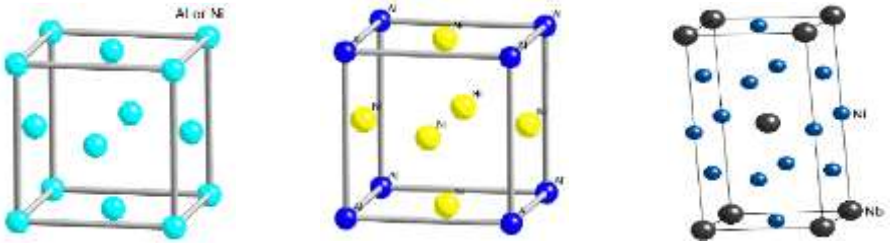

(a) (b) (c)

Fig. 3 Crystal structures of γ (a), γ' (b) and (c) γ'' phases in Ni-based superalloys.

4.2. Gamma double prime, γ''

In which nickel and niobium combine in the presence of iron to form body centered tetragonal (BCT) Ni_3Nb, which is coherent with the gamma matrix, while including large mismatch strains of the order of 2.9%, as shown in **Fig. 3 (c)**. This phase provides very high strength at low to intermediate temperatures, but is unstable at temperatures above about 650 °C (1200 °F). This precipitate is found in nickel-iron alloys **[15].**

4.3. Carbides

The added content of carbon is approximately 0.05-0.2%. In combination with reactive and refractory elements such as titanium, tantalum, and hafnium it forms carbides (e.g., TiC, TaC, or HfC). During heat treatment these carbides begin to decompose and forms lower carbides such as $M_{23}C_6$ and M_6C, which tend to generate on the grain boundaries. The mainly M elements in $M_{23}C_6$ are chromium, iron, tungsten and molybdenum, where as the M elements in M_6C are generally molybdenum, tungsten, chromium, cobalt and tantalum. When $M_{23}C_6$ is formed in the grain boundaries, the chromium content in the matrix is reduced and the solubility for γ´ is increased in these zones **[16].**

MC Carbides

FCC in structure usually forms in superalloys during freezing. They are distributed heterogeneously through the alloy, both in intergranular and transgranular positions, often interdendritically. Little or no orientation relation with the alloy matrix has been noted.

MC carbides are a major source of carbon for subsequent phase reactions during heat treatment and service. In some alloys, such as Incoloy 901 and A286, MC films may form along grain boundaries and reduce ductility.

These carbides, for example, TiC and HfC, are among the most stable compounds in nature. The preferred order of formation (in order of decreasing stability) in superalloys for these carbides is HfC, TaC, NbC, and TiC **[15].**

In these carbides, M atoms can readily substitute for each other, as in (Ti, Nb)C. However, the less reactive elements, principally molybdenum and tungsten, can also substitute in these carbides. For example, (Ti, Mo)C is found in Udimet 500, M-252, and René 77.

It appears that the change in stability order cited above is due to the molybdenum or tungsten substitution, which weakens the binding forces in MC carbides to such an extent, those degeneration reactions.

This typically leads to the formation of the more stable compounds $M_{23}C_6$ and M_6C-type carbides in the alloys during processing or after heat treatment and/or service.

Additions of niobium and tantalum tend to counteract this effect. Recent alloys with high niobium and tantalum contents contain MC carbides that do not break down easily during processing or solution treatment in the range of 1200 to 1260 °C.

$M_{23}C_6$ Carbides

It is readily form in alloys with moderate to high chromium content. They form during lower temperature heat treatment and service (that is, 760 to 980 °C) both from the degeneration of MC carbide and from soluble residual carbon in the alloy matrix.

When tungsten or molybdenum is present, the approximate composition of $M_{23}C_6$ is $Cr_{21}(Mo, W)_2C_6$, although it also has been shown that appreciable nickel can substitute in the carbide. It is also possible for small amounts of cobalt or iron to substitute for chromium.

The $M_{23}C_6$ particles strongly influence the properties of nickel alloys. Rupture strength is improved by the presence of discrete particles, apparently through the inhibition of grain-boundary sliding.

Eventually, however, failure can initiate either by fracture of particles or by decohesion of the carbide/matrix interface. In some alloys, cellular structures of $M_{23}C_6$ have been noted. These can cause premature failures, but can be avoided by proper processing and/or heat treatment **[17].**

M_6C carbides

M_6C carbides have a complex cubic structure. They form when the molybdenum and/or tungsten content is more than 6 to 8 at.%, typically in the range of 815 to 980 °C.

Typical formulas for M_6C are $(Ni, Co)_3Mo_3C$ and $(Ni, Co)_2W_4C$. M_6C carbides are formed when molybdenum or tungsten acts to replace chromium in other carbides; unlike the more rigid $M_{23}C_6$, the compositions can vary widely Because M6C carbides are stable at higher levels than are $M_{23}C_6$ carbides, M_6C is more commercially important as a grain-boundary precipitate for controlling grain size during the processing of wrought alloys **[18].**

Carbide Reactions

MC carbides are a major source of carbon in most nickel-base super alloys below 980 °C. However, MC decomposes slowly during heat treatment and service, releasing carbon for several important reactions.

The principal carbide reaction in many alloys is believed to be the formation of $M_{23}C_6$:

$$\mathbf{MC + \gamma \longrightarrow M_{23}C_6 + \gamma' \text{ or}}$$
$$\mathbf{(Ti, Mo)C + (Ni, Cr, Al, Ti) \longrightarrow Cr_{21}Mo_2C_6 + Ni_3 (Al, Ti)}$$

The carbide M_6C can form in a similar manner.

The dominating formulas for formation of these two carbides are:

$$MC + \gamma \rightarrow M_6C + \gamma' \quad \mathbf{(1)}$$
$$MC + \gamma \rightarrow M_{23}C_6 + \gamma' \quad \mathbf{(2)}$$
$$\mathbf{M_6C + M` \rightarrow M_{23}C_6 + M``} \quad (3)$$

M´ and M´´ can be substituted with chromium cobalt, nickel or molybdenum. All these carbides have a fcc crystal structure and increase the rupture strength at high temperature. Some forms of carbides are shown in **Figure** .

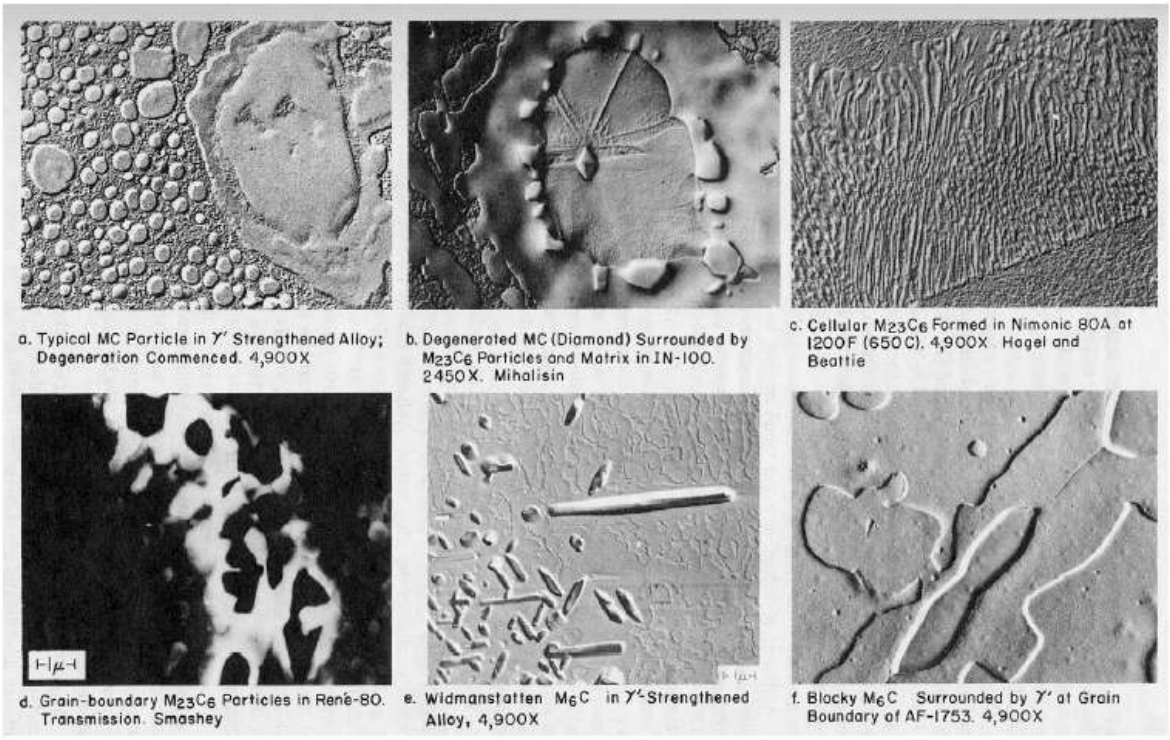

Figure 4 Forms of carbides.

Borides
a relatively low density of boride particles formed when boron segregates to grain boundaries.

Topologically Close-Packed Phases
Close-packed phases are usual undesirable, brittle phases which are formed during heat treatment. The structure of these phases consists of close-packed atoms in layers with relatively large interatomic distances one below the other. The characteristic topology is generated when the layers sandwich larger atoms, shown in **Figure** .

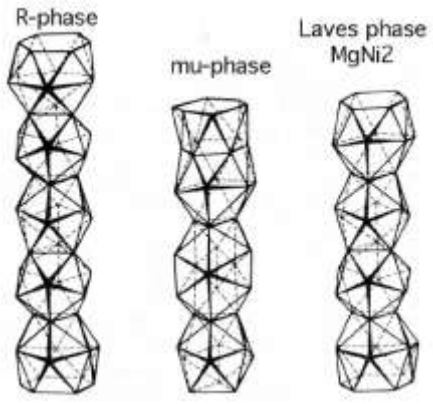

Figure 5 TCP phases. [3]

This structure is called topologically close-packed (TCP). In the opposite the γ′ phase is close-packed in all directions and is called geometrically close-packed (GCP). Alloys containing transition metals, such as tantalum, niobium, chromium, tungsten or molybdenum, are the most violable alloys to the formation of TCP phases, **Fig. 6 [19-23]**.

The common forms of TCPs are σ, μ and Laves. The hard and plate-like σ phase has a composition of the type $(Cr,Mo)_x(Ni,Co)_y$, possesses 30 atoms per cell, the structure is similar to the carbides $M_{23}C_6$ and is the most undesirable form.

Crack initiation caused by the shape and the hardness of the phase leads to brittle failure. The σ phase has also the responsibility for shortened creep rupture life.

The μ phases have a similar composition such the σ phases with a majority of Mo and Co. The structure is similar to the carbides M_6C and possesses 13 atoms per cell.

The Laves phases have a composition of the type AB_2 such as $MoCo_2$ and $TaCo_2$ and a negative influence of tensile ductility and creep properties at room temperature **[24].**

Usually all types have a plate structure which has negative effects to mechanical properties such as ductility and creep-rupture. TCPs are potentially damaging tie up γ and γ′ strengthening elements, thus reducing creep strength, and they can act as crack initiators because of their brittle nature.

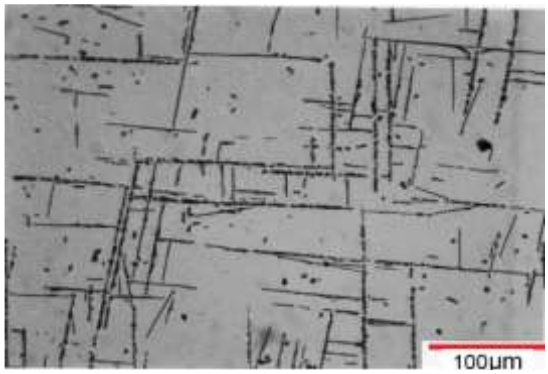

Fig. 6 TCP phases (needle shape) in Ni Base Superalloys.

PROCESSING OF NI BASE SUPERALLOYS

4.4. Melting

Vacuum Induction Melting (**VIM**) is used as the standard melting practice for the preparation of superalloy stock, **Fig. 7**. Raw metallic materials including scrap are charged into a refractory crucible and the crucible is maintained under a vacuum during melting of the charge. Typically, more than 30 elements are refined or removed from the superalloy melt during VIM processing. The main advantages of melt treatment under vacuum can be summarized as follows **[25]:**

1. Extensive degassing of melts (eg, hydrogen < 1ppm).
2. Significant reduction of non-metallic inclusions (oxides, nitrides) compared to melting under air.
3. Deoxidation by carbon (down to low levels of oxygen) without formation of solid or liquid reaction products.
4. Ability to manufacture very low carbon high strength steels or superalloys.
5. Evaporation of trace elements.

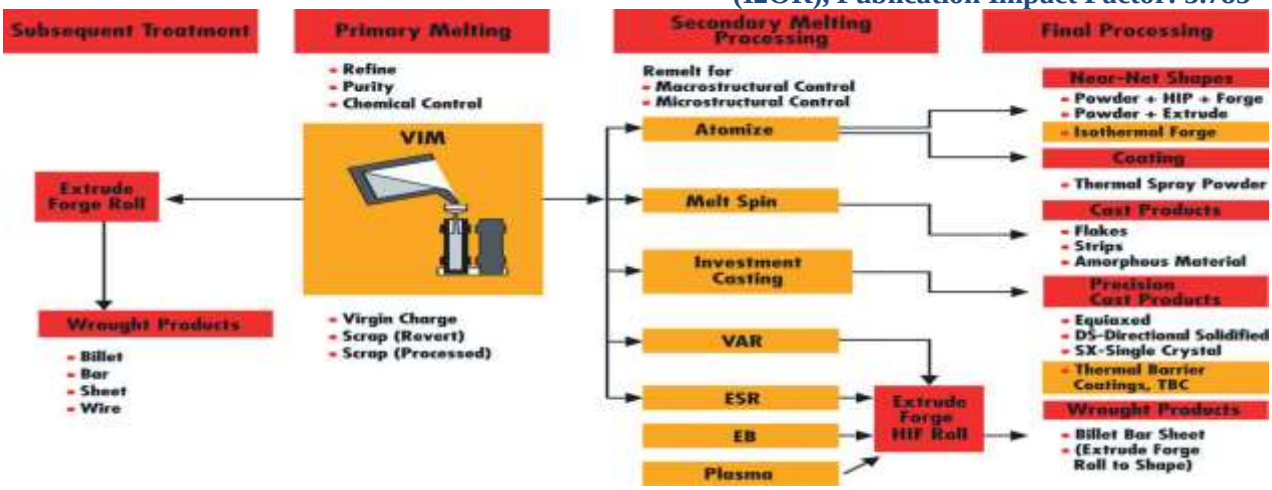

Fig. 7 Processing routes for superalloys.

The VIM or Vacuum Induction Melting Degassing and Pouring (VIDP) furnace is the central core of every vacuum refining operation. Here, melting, refining and alloying are done under controlled conditions. With melting capacities from a few kilograms up to 30t, VIM/VIDP furnaces offer a wide range. For smaller weights (5–500kg) VIM is the preferred melting tool; for larger charge weights (above 2t) VIDP is the most suitable furnace type. In this unique vacuum melting system the crucible itself acts as the vacuum melt chamber. VIDP furnaces provide faster pump down compared with chamber-type VIMs of the same melting capacity, because of the dramatically reduced chamber volume **[26].**

Investment casting

Development of new blade alloys to achieve high temperature performance has required parallel development in alloy processing. Before the 1940s, gas turbine engine blades were iron-based alloys through cold wrought. In the 1940s and 1950s, investment casting and vacuum melting were introduced to manufacture engine blades. In the 1970s, the directional solidification (DS) process was invented and made a great advance in the thermal capability of the blades. The grain boundaries were significantly decreased and the crystals were all aligned in the direction of centrifugal stress. Based on the DS casting process, single crystal (SX)

blades were exploited, which are free from high angle grain boundaries and therefore dramatically increase the melting point of turbine blades **[27-31].** To date, all the modern Trent family of engines incorporate single crystal materials. Nowadays, turbine blades are designed with complex geometries and intricate channels which allow cooler air flow within and along the blades during operation **[32, 33].** Therefore, turbine components are usually produced by investment casting.

As shown in **Fig. 8**, the investment casting process (also called lost-wax casting) involves the following steps:

1. A pattern of the component of the casting is prepared by injecting molten wax into a metal mould. If necessary (such as for cooling passages in turbine blades), ceramic cores can be prefixed into the mould to intricate hollows for the castings. Wax patterns can be assembled in clusters to enable several blades to be produced in a single casting.

2. The wax mould is then dipped into ceramic slurry consisting of binding agents and mixtures of zircon ($ZrSiO_4$), alumina (Al_2O_3) and silica (SiO_2), followed by stuccoing with larger particles of the above materials. This process needs to be repeated several times until the shell thickness is thick enough to withstand the mechanical shock of receiving the molten metal.

3. After the shell is constructed, the wax is removed in an autoclave or furnace.

4. The ceramic mould is then fired to high temperature to build up its strength and make it ready to receive the molten superalloy.

5. When the casting is finished, the investment shells are knocked off and the ceramic cores are leached out using a high-pressure autoclave by chemical means.

ISSN: 2277-9655
(I2OR), Publication Impact Factor: 3.785

Fig. 8 Illustration of the various stages of investment casting process.

Advantages:

- Parts of great complexity and intricacy can be cast.
- Close dimensional control and good surface finish.
- Wax can usually be recovered for reuse.
- Additional machining is not normally required - this is a net shape process.

Disadvantages

- Many processing steps are required.
- Relatively expensive process.

Investment Casting Defects

Distortion, poor surface finish (fins / spines, nodules, veins and ridges, and rough surface), porosity, voids, incomplete castings.

Figure 9 illustrates the investment casting furnace for single crystal turbine blades. Based on directional solidification (DS), the molten alloy is poured into a hot ceramic mould at a temperature of approximately 1500˚C, which is maintained by radiant heating in the furnace. A water-cooled copper chill plate is located at the bottom to make the solidification start at the bottom. During solidification, the solid-liquid growth front can be controlled by heat flow in the mould. By slowly withdrawing the mould out of the furnace, metal solidifies directionally from bottom to top,

producing large, columnar grains which are elongated in the direction of withdrawal, markedly improving the creep properties. In single crystal (SX) castings, to entirely remove the transverse grain boundaries, a grain selector is added at the base of the mould. As a result, only one grain with a preferred orientation can eventually survive at the top of the grain selector and grow into the main body of the turbine blades, which allows free of high angle boundaries (HABs) in SX superalloys. Since HABs are preferential sites for crack initiation, creep resistance of SX alloys can be dramatically improved. Depending on the size of the blade, the entire process takes 3-6 hours to complete.

To further control the quality of the single crystal turbine blades, particular attention has been paid to grain selectors. Different designs of grain selector are employed as shown in **Fig. 10**. The most common type is the spiral grain selector which is often known as the "pig-tail" grain selector **(Fig.10 (b)) [34]**.

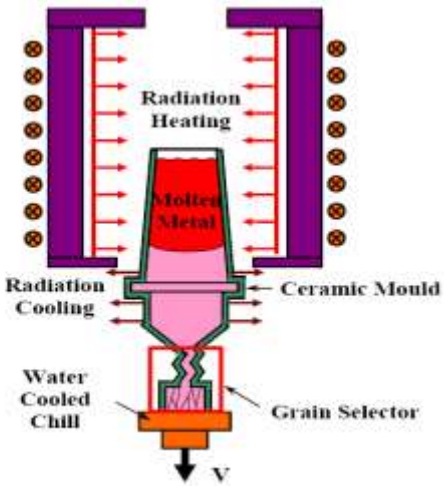

Fig. 9 Schematic illustration of investment Single crystal turbine blades.

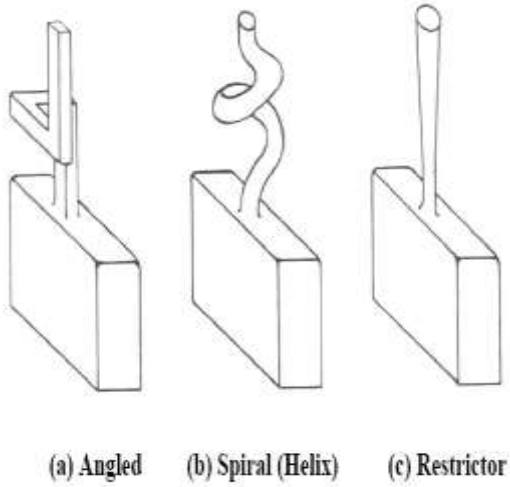

Fig. 10 Various designs of grain selector for casting for SX turbine blades.

DEVELOPMENT IN NI BASE SUPERALLOYS

The developments in superalloy processing have brought about considerable increases in superalloy operating temperatures. Superalloys were originally iron based and cold wrought prior to the 1940s. In the 1940s investment casting of cobalt base alloys significantly raised operating temperatures. The development of vacuum melting in the 1950s allowed for very fine control of the chemical composition of superalloys and reduction in contamination and in turn led to a revolution in processing techniques such as directional solidification of alloys and single crystal superalloys **[35].**

Single-crystal superalloys (SC superalloys) are formed as a single crystal, so there are no grain boundaries in the material. The mechanical properties of most other alloys depend on the presence of grain boundaries, but at high temperatures, they would participate in creep and must be replaced by other mechanisms. In many such alloys, islands of an ordered intermetallic phase sit in a matrix of disordered phase, all with the same crystalline lattice. This approximates the dislocation-pinning behavior of grain boundaries, without introducing any amorphous solid into the structure.

The material and casting technique improvements that have taken place during the last 50 years have enabled superalloys to be used first as equiaxed castings in the 1940s, then as directionally solidified (DS) materials during the 1960s, and finally as single crystals (SC) in the 1970s. Each of these casting techniques advancement has resulted in higher use temperatures, as shown in **Fig 11 [34]**.

6.1. Directional solidification process

In DS processing, columnar grains are formed parallel to the growth axis. In nickel-based alloys, the natural growth direction is along the <100> crystallographic direction. Solidification first occurs at the bottom plate, after which the mold is slowly withdrawn from the furnace, allowing the metal inside to directionally solidify from bottom to top.

One of the first directionally solidified alloys developed was MarM200Hf. The Hf addition contributes to preventing intergranular cracking during the directional solidification. A similar improvement was made too many other typical Conventional Casting (CC) alloys such as Rene80DS, GTD111DS and MarM247DS. TMS was the strongest among the first generation alloys, with strength equivalent to that of the present second generation DS alloys. Mitsubishi Heavy Industries uses their original superalloys MGA1400 and MGA 2400 for the blades and

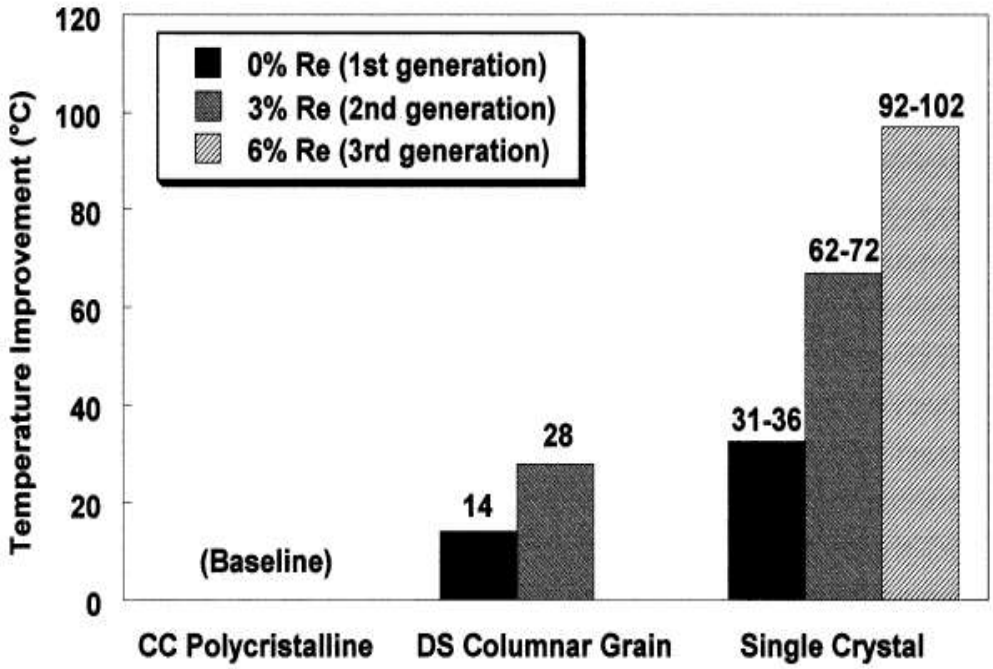

Fig. 11 Typical temperature advantages over CC superalloys obtained with DS and SX superalloys estimated from stress rupture tests performed at 982˚C and 248MPa.

vanes of a 1500ºC-class large gas turbine that was put to practical use in 1999 **[36, 37].** **Figure 12** shows the difference in structure between the CC, DS and SC turbine blades.

Second generation DS alloys contain 3wt% Re, which enhance the solid solution strengthening of the γ phase and has a creep strength equivalent to that of first generation SC alloys. CM186C and Rene 142 are typical DS alloys widely used in jet engines.

TMD 103, developed in NIMS is the first third generation (6wt%Re) DS alloy, developed by converting a third generation SC alloy into a DS alloy by adding the grain boundary strengthening elements, carbon and boron. This alloy has a creep strength equivalent to that of the second generation SC alloy CMSX-4. Table 1 contains different chemical compositions of Ni based superalloys used for turbine blades of CC, DS and SC **[38].**

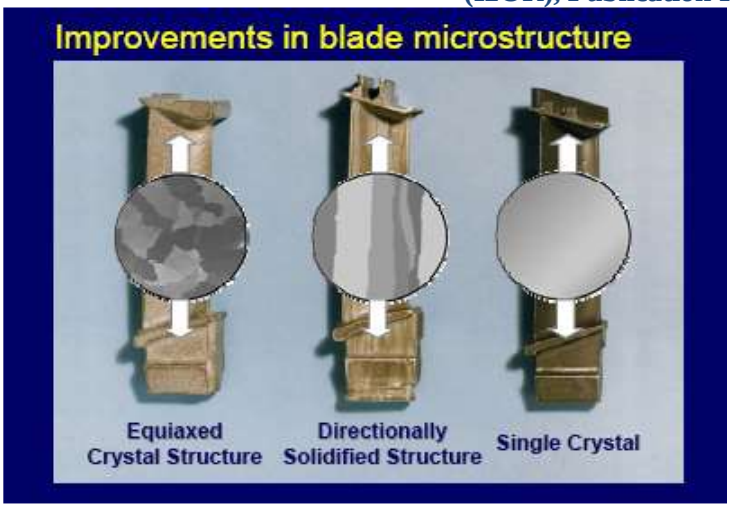

Fig. 12 Structure of Polycrystalline (CC), Directional Solidified (DS) and Single Crystal (SC). [32]

Single crystal process

The chemistry of the Ni-based superalloys designed for single crystal (SC) gas turbine blades has significantly evolved since the development of the first generation of alloys derived from columnar grained materials. The overall performance of the second and third generations has been significantly improved by the addition of increasing amounts of rhenium. However, the problems of increased density, grain defects and microstructural stability have also become more and more acute and render necessary to carefully control the level of the various alloying elements in order to effectively benefit from the high potential of the most recently developed third generation alloys ***[39].***

First generation alloys

The alloying elements in the first generation Ni Based single crystal superalloys are mainly Cr, Co, Mo, W, Al, Ti, Ta and sometimes Nb or V. Cr, Co, Mo partition preferentially to the austenitic face centered cubic nickel-based matrix where they act mainly as solid solution strengthening elements. Cr also plays an essential role in the hot corrosion resistance since it promotes the formation of a protective Cr_2O_3 oxide scale.

The elements Ti, Ta, Nb and V strengthen the γ′ precipitates by substituting to Al in Ni_3Al. Al also plays a fundamental role in promoting the formation of a stable Al_2O_3 alumina surface scale which protects the alloy against further oxidation.

Alloy NASAIR 100 was derived from Mar-M247 essentially by suppressing these grain boundary strengthening elements **[40].** This leading to an increase in incipient melting temperature from 1240 to 1330°C, which allowed a complete solutioning of the secondary γ′ precipitates. The resulting increase in creep strength was shown to be equivalent to a 58°C temperature advantage at high temperatures and low stresses **[40-43].**

One great advantage of the first generation SC superalloy, NASAIR 100, compared to CC and DS alloys is the possibility to achieve a homogeneous microstructure using a single high temperature heat treatment, which allowed the elimination of almost all the γ/γ′ eutectic interdendritic nodules and solutioning of all the secondary γ′ precipitates.

The pioneering work on CMSX-2 has shown that the creep behavior of high γ′ volume fraction alloys can be optimized by choosing a precipitation heat treatment leading to cubical γ′ precipitates with a mean cube edge of approximately 0.45 μm **[44].**

Second generation alloys

The addition of rhenium (Re) at the expense of other refractory elements as W or Ta made a significant improvement of the creep strength of the SC superalloys. Re substantially lowers the γ′ coarsening kinetics, leads to a large negative

γ-γ′ misfit. In addition, Re forms atom clusters within the γ matrix of these alloys, which is a more potent source of strengthening than the conventional solid solution effect **[44].** The temperature capability of the first SC superalloys was improved by about 30°C by adding 3wt% of Re labeled as second generation superalloys. Re also contributes positively to the hot corrosion and oxidation resistance. Some examples of these alloys are PWA1484, Rene N5 and CMSX-4 **[45].**

However, Re has some deleterious effects on microstructure stability and mechanical properties. Re in superalloys increases the propensity to form undesirable topologically close-packed (TCP) brittle phases as μ, σ or P during exposure at high temperature. These TCP phases decrease the impact strength, ductility or creep strength. In SC superalloys containing high levels of Re and W sometimes a casting defect called freckles could occur. These freckles form due to the convection instabilities resulting from solute partitioning that lowers the density of the liquid in the mushy zone. This defect can be cured by increasing the level of Ta which is rejected to the interdendritic areas lowering the density inversions **[46].**

Third generation alloys

Third generation of SC superalloys started with increasing the Re content to 6Wt% Re aiming to improve the temperature capability of these alloys. The challenge was to achieve improved creep strength, without increasing the density and by keeping the alloy not too much prone to the precipitation of TCP phases. Examples of this group of alloys include CMSX-10 and Rene N6. Ruthenium (Ru) was introduced by General Electric (GE) to third generation SC as a recent improvement. **Table 1** shows the nominal composition of some cast Ni base superalloys.

The tendency to the precipitation of TCP phases in the third generation is more important problem than in second generation alloys. The Cr level in third generation is decreased than in second generation to 2 - 4.2% to keep the alloys less prone to TCP phase precipitation. Third generation SC superalloys containing some additions of Ru or Ir seem to show a reduced tendency to form undesirable TCP phases, these alloys exhibit excellent creep strength, especially at higher temperatures.

A great advantage of the third generation SC superalloys is that they maintain a rather high creep resistance at temperature above 1100°C. Indeed, the stress rupture life at 1150°C and 100 MPa of the MC-NG alloy is over 150 hrs, whereas the first generation alloys show, typically, a rupture life less than 10 hrs **[47].**

Table 1 Nominal composition of cast Ni base superalloys.

Process	Alloy	Composition (wt%, Ni balance)														Generation
		Co	Cr	Mo	W	Al	Ti	Nb	Ta	Hf	Re	C	B	Zr	Others	
CC	IN 738	8.5	16	1.7	2.6	3.4	3.4	–	1.7	–	–	0.17	0.01	0.1	–	–
	IN 792	9	12.4	1.9	3.8	3.1	4.5	–	3.9	–	–	0.12	0.02	0.2	–	–
	Rene'80	9.5	14	4	4	3	5	–	–	–	–	0.17	0.015	0.03	–	–
	MarM247	10	8.5	0.7	10	5.6	1	–	3	–	–	0.16	0.015	0.04	–	–
	TM-321	8.2	8.1	–	12.6	5	0.8	–	4.7	–	–	0.11	0.01	0.05	–	–
DS	GTD111	9.5	14	1.5	3.8	3	4.9	–	2.8	–	–	0.1	0.01	–	–	1st
	MGA1400	10	14	1.5	4	4	3	–	5	–	–	0.08	?	0.03	–	1st
	CM247LC	9	8	0.5	10	5.6	0.7	–	3.2	1.4	–	0.07	0.015	0.01	–	1st
	TMD-5	9.5	5.8	1.9	13.7	4.6	0.9	–	3.3	1.4	–	0.07	0.015	0.015	–	1st
	PWA1426	12	6.5	1.7	6.5	6	–	–	4	1.5	3	0.1	0.015	0.03	–	2nd
	CM186LC	9	6	0.5	8.4	5.7	0.7	–	3.4	–	3	0.07	0.015	0.005	–	2nd
	TMD-103	12	3	2	6	6	–	–	6	0.1	5	0.07	0.015	–	–	3rd
	TMD-107	6	3	3	6	6	–	–	6	0.1	5	0.07	0.015	–	2Ru	4th
SC	PWA1480	5	10	–	4	5	1.5	–	12	–	–	–	–	–	–	1st
	Rene'N4	8	9	2	6	3.7	4.2	0.5	4	–	–	–	–	–	–	1st
	CMSX-2	4.6	8	0.6	8	5.6	1	–	9	–	–	–	–	–	–	1st
	TMS-6	–	9.2	–	8.7	5.3	–	–	10.4	–	–	–	–	–	–	1st
	MC2	5	8	2	8	5	1.5	–	6	–	–	–	–	–	–	1st
	MDSC-7M	4.5	10	0.7	6	5.4	2	–	5.4	–	0.1	–	–	–	–	1st
	TMS-26	8.2	5.6	1.9	10.9	5.1	–	–	7.7	–	–	–	–	–	–	2nd
	PWA1484	10	5	2	6	5.6	–	–	9	–	3	–	–	–	–	2nd
	Rene'N5	8	7	2	5	6.2	–	–	7	0.2	3	–	–	–	–	2nd
	CMSX-4	9	6.5	0.6	6	5.6	1	–	6.5	0.1	3	–	–	–	–	2nd
	TMS-82+	7.8	4.9	1.9	8.7	5.3	0.5	–	6	0.1	2.4	–	–	–	–	2nd
	YH 61	1	7.1	0.8	8.8	5.1	–	0.8	8.9	0.25	1.4	0.07	0.02	–	–	2nd
	Rene'N6	12.5	4.2	1.4	6	5.75	–	–	7.2	0.15	5.4	0.05	0.004	–	0.01Y	3rd
	CMSX-10	3	2	0.4	5	5.7	0.2	0.1	8	0.03	6	–	–	–	–	3rd
	TMS-75	12	3	2	6	6	–	–	6	0.1	5	–	–	–	–	3rd
	MC 653	–	4	1	6	5.3	1	–	6.2	0.1	5	–	–	–	3Ru, 0.1Si	4th
	TMS-138	5.8	2.8	2.9	6.1	5.8	–	–	5.6	0.05	5.1	–	–	–	1.9Ru	4th
	TMS-162	5.8	2.9	3.9	5.8	5.8	–	–	5.6	0.09	4.9	–	–	–	6.0Ru	4/5th
ODS	MA6000	2	15	2	4	4.5	2.5	–	2	–	–	0.05	0.01	0.15	1.1Y2O3	–
	TMO-20	8.7	4.3	1.5	11.6	5.5	1.1	–	6	–	–	0.05	0.01	0.05	1.1Y2O3	–

Fourth generation alloys

4th generation Ni-base superalloys contain 2–3 wt% Ru, which hinders the precipitation of topologically close packed (TCP) phases **[48]** and improves the high-temperature microstructure stability **[49-51].** 4th generation superalloys have achieved temperature capabilities 30°C higher on average than those of the previous generation superalloys in terms of high-temperature creep strength. **Table 2** shows Some examples of 2nd, 3rd and 4th generations of Ni based super alloys compositions (wt%), associated with alloy density ρ (g/cm^3) estimated by NIMS alloy design program.

Fifth generation alloys

5th generation superalloys have been invented by the optimization of alloying compositions, and the content of Ru has increased to 5–6wt%; the lattice misfit between the γ and the γ' phases has been controlled to balance the interfacial strengthening and coherency, and the dislocation network at the interface of the γ and the γ' phases has become finer than that of 4th generation superalloys in order to inhibit dislocation migration under stress. Thus, the high-temperature creep resistance of 5th generation superalloys is better than that of 4th generation superalloys **[52]**.

However, these 4th and 5th generations of superalloys are likely to have lower resistance against oxidation than the previous generations owing to the higher content of refractory elements such as Mo, Re and Ru **[53, 54]**. These refractory-based oxide species have relatively higher vapor pressures and can disrupt the continuity of protective Al_2O_3 formed on the surface during thermal exposure. To make 4th and 5th generation superalloys commercially viable, an improvement in oxidation resistance is imperative.

Table 2 Some examples of 2nd, 3rd, 4th and 5th generations of Ni based super alloys compositions (wt%), associated with alloy density ρ (g/cm^3) estimated by NIMS alloy design program

Alloy Generations		Cr	Co	Mo	W	Al	Ti	Ta	Hf	Re	Ru	ρ
2nd	CMSX-4	6.5	9.0	0.6	6.0	5.6	1.0	6.5	0.1	3.0	-	8.70
	PWA1484	5.0	10.0	2.0	6.0	5.6	-	9.0	0.1	3.0	-	8.95
	Rene' N5	7.0	8.0	2.0	5.0	6.2	-	7.0	0.2	3.0	-	8.63
3rd	Rene' N6	4.2	12.5	1.4	6.0	5.75	-	7.2	0.15	5.4	-	8.98
	CMSX-10	2.0	3.0	0.4	5.0	5.7	0.2	8.0	0.03	6.0	-	9.05
	TMS-75	3.0	12.0	2.0	6.0	6.0	-	6.0	0.1	5.0	-	8.89
4th	MX-4/PWA1497	2.0	16.5	2.0	6.0	5.6	-	8.3	0.15	6.0	3.0	9.20
	MC-NG	4.0	0	1.0	5.0	6.0	0.5	5.0	0.1	4.0	4.0	8.75
	TMS-138	3.2	5.8	2.9	5.9	5.8	-	5.6	0.1	5.0	2.0	8.95
	TMS-138A	3.2	5.8	2.9	5.6	5.7	-	5.6	0.1	5.8	3.6	9.01
5th	TMS-162	3.0	5.8	3.9	5.8	5.8	-	5.6	0.1	4.9	6.0	9.04
	TMS-173	3.0	5.6	2.8	5.6	5.6	-	5.6	0.1	6.9	5.0	9.11
	TMS-196	4.6	5.6	2.4	5.0	5.6	-	5.6	0.1	6.4	5.0	9.01

Sixth generation alloys

A 6th generation superalloy, TMS-238, which exhibits both high-temperature creep strength and improved oxidation resistance, has been developed. The alloy design procedure involves utilizing the composition of TMS-196 **[55]** as a base to optimize the alloy chemistry so as to improve the oxidation resistance and creep strength. High-temperature

properties such as creep, oxidation and hot-corrosion resistances have been iproved for this new superalloy; the experimental results have been compared with those of a 2nd generation superalloy CMSX-4 and a 4th generation superalloy MX- 4/PWA1497. **Table 3** shows the nominal compositions (wt% Ni bal.) for sixth generation TMS-238 alloys.

Table 3. Nominal composition (wt% Ni bal.)

Alloy	Co	Cr	Mo	W	Al	Ti	Ta	Hf	Re	Ru
TMS-238	6.5	4.6	1.1	4.0	5.9	0.0	7.6	0.1	6.4	5.0

The oxidation property was investigated and is shown in **Fig. 13**. TMS-196 showed an improvement over TMS-138A and has excellent oxidation resistance compared with other 4th and 5th generation superalloys [11]: however, it shows a large decrease in mass in the cyclic oxidation test because of scale spallation, and the oxidation resistance is still inferior to CMSX-4. CMSX-4 shows a relatively stable profile but a slight decrease in mass is found after 50 cycles. Interestingly, TMS-238 shows a constant and gentle increase in mass change until 500 cycles and above.

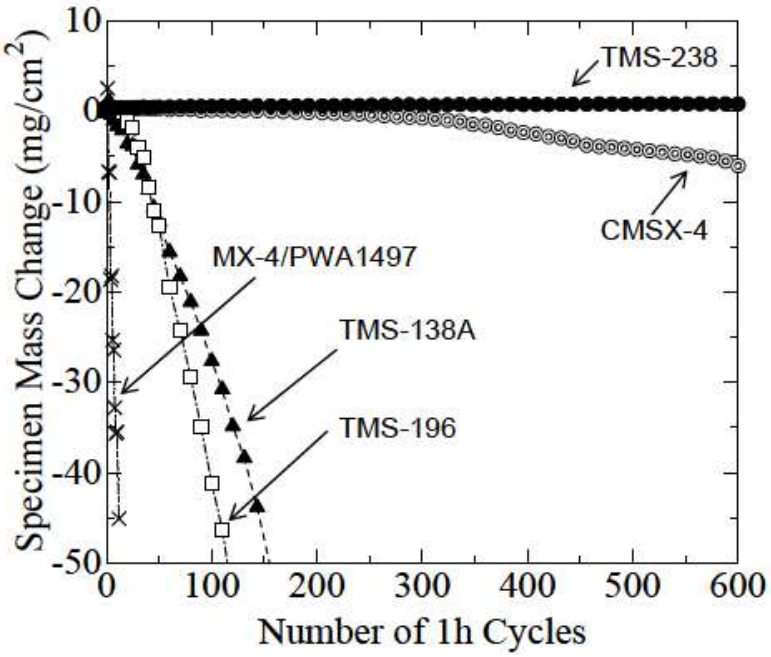

Fig. 13 Results of 1100 °C cyclic oxidation tests.

Figure 14 shows the metal losses of CMSX-4, TMS-138A, TMS-196 and TMS-238 after 20 h of soaking. TMS-238 had by far the lowest metal loss; hence, this alloy exhibits the best hot-corrosion resistance. It is likely that a lower Mo content and a higher Re content are responsible for this excellent property.

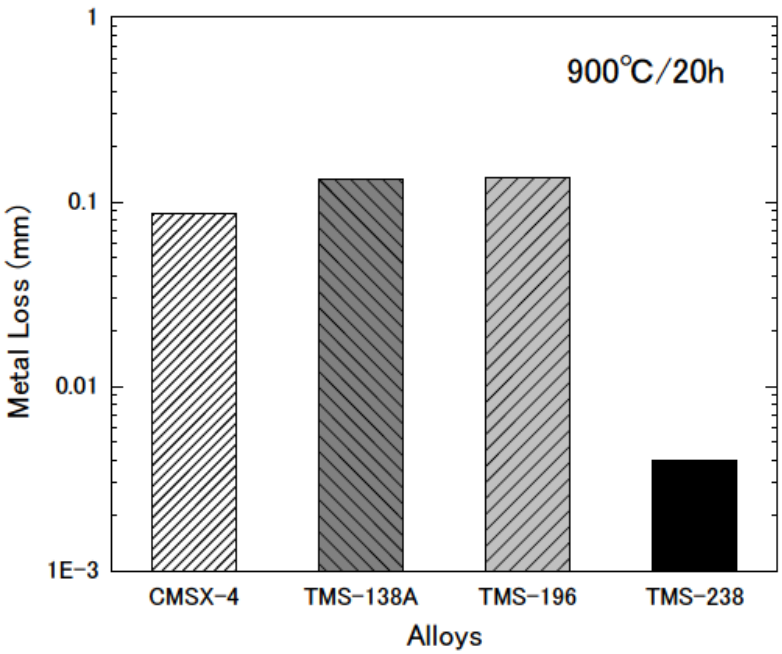

Fig. 14 Results of hot corrosion tests.

Figure 15 shows the relationship between creep property and the oxidation resistance. The vertical axis is the oxidation resistance at 1100°C, which was originally defined as including the factors of isothermal mass increase and cyclic mass decrease, and it is expressed as:

$$\text{Oxidation Resistance} = \log\left(\frac{1}{w_1} \times \frac{1}{|w_{50} - w_1|}\right)$$

where $w1$ is mass gain after the 1st cycle and $w50-w1$ is the mass change from the 1st cycle to the 50th cycle in a 1100°C cyclic oxidation test. In this equation, $1/w1$ is the isothermal oxidation resistance and a $1/|w50-w1|$ is the cyclic oxidation resistance. A larger value means better durability in both factors, and so the total oxidation resistance is expressed as the increase in the value in the vertical axis in **Fig. 15.** The horizontal axis indicates the rupture life (h) in the creep test at 1100°C/137 MPa. The open squares, diamonds, triangles and inverted triangles are symbols representing commercial 1st, 2nd, 3rd and 4th generation superalloys.

The solid inverted triangle, solid circle and solid double circle stand for NIMS 4th, 5th and 6th generation superalloys. Superalloys were developed focusing on only their mechanical properties up to 4th generation, as shown by the gray arrows in the figure.

However, the solid circle and the solid double circle in **Fig. 15** show that superalloys with good oxidation resistance and mechanical properties are being developed owing to the recent efforts to improve the oxidation resistance of these alloys. It is evident that TMS-238 has excellent mechanical and environmental properties and that these are in good balance with each other.

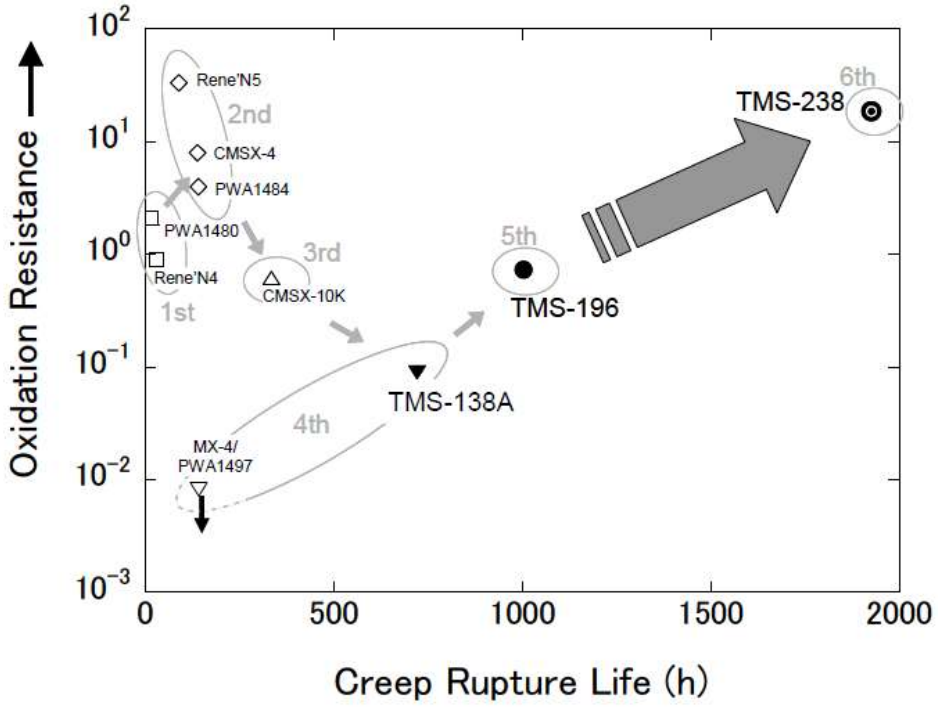

Fig. 15 Graph showing comarisons among alloys in terms of a combination of 1100 °C/137 Mpa creep and 1100 °C oxidation.

EFFECT OF ALLOYING ELEMENTS IN NI BASE SUPERALLOYS

Commercial Nickel Based Superalloys include more than just Ni. Most nickel-based alloys contain 10-20% Cr, up to 8% Al and Ti, 5-10% Co, and small amounts of B, Zr, and C. Other common additions are Mo, W, Ta, Hf, and Nb. The elemental additions in Ni-base superalloys can be categorized as being

a) γ formers (elements that tend to partition to the γ matrix)
b) γ' formers (elements that tend to partition to the γ´ precipitate)
c) carbide formers
d) Elements that segregate to the grain boundaries.

The γ formers can be found in Group V, VI, and VII and are elements such as Co, Cr, Mo, W, Fe. The difference between these elements and Ni (the primary matrix element) are only 3-13% concerning the atomic diameters. γ formers come from group III, IV, and V elements and include Al, Ti, Nb, Ta, Hf. The atomic diameters of these elements differ from Ni by 6-18%. The main carbide formers are Cr, Mo, W, Nb, Ta, Ti, **Fig. 16**. The carbides precipitate at grain boundaries and reduce the tendency for grain boundary sliding **[56].** Elements which stabilize the grain boundary are B, C, and Zr. Their atomic diameters differ from Ni by 21-27%. The resulting reduction in grain boundary energy is associated with better creep strength and ductility.

Chromium and aluminium are necessary for oxidation resistance. A small amount of yttrium binds the oxide layer to the substrate.

The elements such as C, Cr, Mo, W, C, Nb, Ta, Ti and Hf form carbides. The elements cobalt, iron, chromium, niobium, tantalum, molybdenum, tungsten, vanadium, titanium and aluminium are also solid-solution strengtheners, both in γ and γ' phase **[46].**

The presence of boron, zirconium and hafnium may modify the initial grain boundary carbides or tie up unwanted elements such as sulphur and lead. Grain boundary diffusion rates are reduced. Otherwise hafnium contributes to the formation of γ-γ`eutectic in cast alloys to improve the ductility.

Limits of the alloying contents exist certainly to avoid undesirable precipitation such as the embrittling phases Laves and Sigma. As shown in **Figure 16**, the alloying elements effects in nickel based superalloys are presented and the "M" indicates the metal atoms.

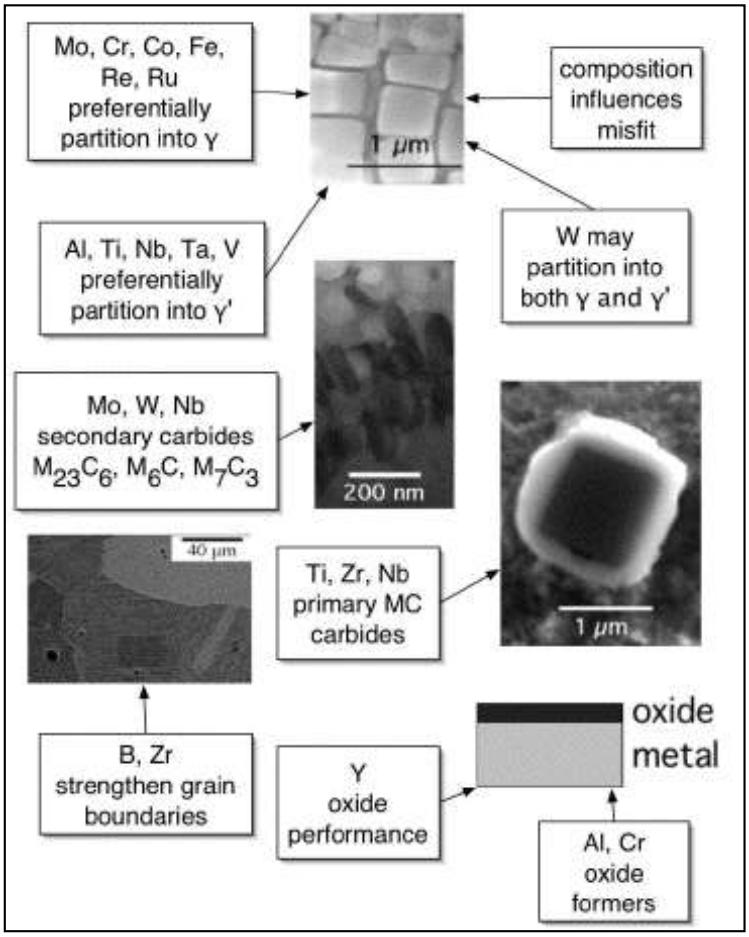

Fig. 16 Effect of various alloying elements in Ni base superalloys.

The abbreviations MA/ODS/PM stand for mechanically alloyed, oxide dispersion- strengthened and powder metallurgical origin.

The single-crystal superalloys (SX) can be classified into first, second and third generation alloys. The second and third generations contain about 3 wt% and 6 wt% of rhenium, which is a very expensive addition but leads to an improvement in the creep strength. It is supposed that the higher resistance to creep comes from the promotion of rafting by rhenium, which partitions into the γ and makes the lattice misfit more negative. Rhenium reduces also the overall diffusion rate in nickel based superalloys, as shown in **Table 4**.

The addition of rhenium promotes TCP formation, so alloys containing these solutes must have their Cr, Co, W or Mo concentrations reduced to compensate **[57, 58].**

In general it is not practically to remove all these elements, but the chromium concentration in the new generation superalloys is more reduced. Chromium does protect against oxidation, but oxidation can also be prevented by coating the blades.

Table 4. Commercial Nickel Based Superalloys.

Alloy		Cr	Co	Mo	W	Ta	Nb	Al	Ti	Fe	C	B	Zr	Re	Hf	Others
Astroloy	PM	14.9	17.2	5.1				4	3.5		0.03		0.04			
CMSX2	SX	8	4.6	0.6	7.9	5.8		5.6	0.9							
CMSX4	SX	5.7	11	0.42	5.2	5.6		5.2	0.74					3	0.1	
CMSX6	SX	9.8	5	3		2.1		4.8	4.7							
CMSX10	SX	2	3	0.4	5	8	0.1	5.7	0.2					6	0.03	
FT750DC	wrought	20			3.5			2.3	2.1	5	0.07	0.005				0.4 Si
Hastelloy X	wrought	22	1.5	9	6					18.5	0.1					0.5Mn, 0.5Si
Hastelloy S	wrought	15.5		14.5				0.2		1	0.02	0.009				0.02 La
Inconel 600	wrought	15.8								7.2	0.04					0.2Mn, 0.2 Si
Inconel 718	wrought	18.6		3.1			5	0.4	0.9	18.5	0.04					0.2Mn, 0.3Si
MA758	MA/ODS	30			0.5			0.3			0.05					0.6 yttria
MA760	MA/ODS	19.5			3.4			6		1.2	0.06					1.0 yttria
MA6000	MA/ODS	15			3.9			4.5	2.3	1.5	0.06					1.1 yttria
MAR-M200	cast	9	10		12		1	5	2		0.15	0.015	0.05			
Nimonic 80A	wrought	19.5	1.1					1.3	2.5			0.06				
Nimonic 105	wrought	14.5	20	5					1.2	4.5		0.2				
PM1000	MA/ODS	20						0.3	0.5	3						0.6 yttria
Rene N5	SX	7	8	2	5	7		6.2						3	0.2	
Rene N6	SX	4.2	12.5	1.4	6	7.2		5.75						5	0.15	
Rene 41	wrought	19	11	10				1.5	3.1		0.09	0.05				
RR2000	SX	10	15	3				0.05	4							1 V
SRR99	SX	8.5	5		9.5	2.8		5.5	2.2							
TMS 63	SX	6.9		7.5		8.4		5.8	0							
Udimet 500	wrought	18	18.5	4				2.9	2.9		0.08	0.006	0.05			
Udimet 700	wrought	15	18.5	5.2				4.3	3.5		0.08	0.03				
Waspaloy	wrought	19.5	13.5	4.3				1.3	3		0.08	0.006	0.06			

STRENGTHENING MECHANISMS IN NI BASE SUPERALLOYS

8.1 The γ mixed – crystal

The face–centered γ-mixed crystal is being hardened trough the elements Co, Fe, Cr, Nb, Ta, Mo and W, as shown in **Fig. 17**. Other solution – hardening elements are Ti, Al, Hf and Zr.

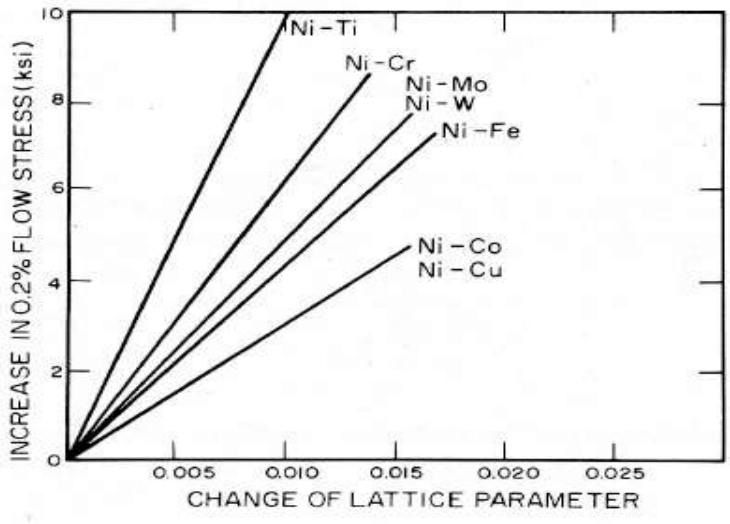

Figure 17 Dependence between yield-stress and change of lattice parameter.

As we can see here, the best improvement will be achieved with Ti. The γ-lattice parameter can be calculated with the following equation **[59].**

$$a_\gamma = 3{,}524 + 0{,}7C_{Ta} + 0{,}7C_{Nb} + 0{,}478C_{Mo} + 0{,}444\,C_W + 0{,}441C_{Re} + 0{,}422C_{Ti} + 0{,}3125C_{Ru} + 0{,}11\,C_{Cr} + 0{,}0196\,C_{Co} \quad (4)$$

a_γ in Å ; C_i in atom-parts in the γ-mixed crystal

The γ ´ precipitate

As we know, creep resistance depends on slowing down the speed of dislocations within the crystal structure. The gamma prime phase [$Ni_3(Al,Ti)$] presents a barrier to dislocations. Strengthening by γ´ is particularly related with the volume fraction (V_f) of γ´ and with the γ´ particle size. In **Fig**Error! Reference source not found. **18** the strength in dependence of the particle size is shown **[59].**

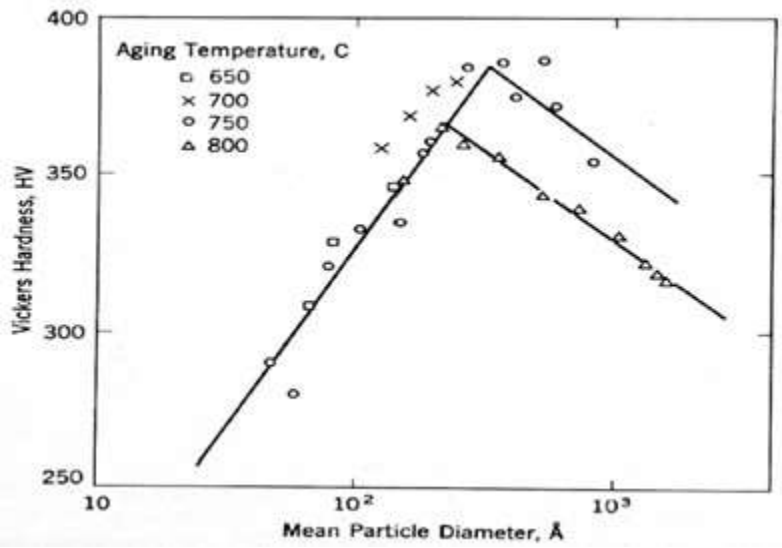

Figure 18 Hardness vs particle diameter.

The main strengthening mechanism is cutting of γ´ particles by dislocations until the hardness peak is attained. As a result the strength increases with the γ´size. After the peak is achieved the strength decreases with the particle size because the dislocations don't cut the γ´ particles but bypass them.

As we said the strength increases also with increasing volume fraction of γ´.Solutes such as aluminum and titanium support the creation of the gamma prime phase.

To achieve highest strengthening in γ´ strengthened alloys, it is essential to heat treat the alloys above the γ´ solvus temperature.

A following aging treatment improves the γ´ distribution and promotes transitions in other phases such as carbides.

Carbide Precipitation (Grain Boundary Strengthening)

Carbides such as $M_{23}C_6$ are formed at the grain boundaries after a heat treatment or an aging process **[60].** This carbides prevent grain boundary sliding and therefore the creep rupture life is improved.

A negative effect of carbide precipitation is the formation of the γ´-precipitate-free zones nearby the grain boundaries. The deformation is concentrated in these regions and there occur consequently the first cracks.

8.4 γ " Precipitation

The precipitation of γ" occurs only in nickel based superalloys with nobium additions, for instance the alloy Inconel 718.

The composition of the γ" is Ni_3Nb or Ni_3V. The particles of γ" appear in forms of discs with the orientation $(001)_{\gamma''}||\{001\}_{\gamma}$ and $[100]_{\gamma''}||<100>_{\gamma}$.

In case that the γ´ and γ´´ phases are existing, the γ´´ phase is the predominant strengthening agent.
γ´´ is easily formable at moderate temperatures after a prior solutioning by heat treatment. Therefore the alloy can be aged after a welding process to generate completely the strengthened structure with adequate ductility.
The γ´´ phase is not a stable phase. After a certain period the γ´´ phase can be converted into a γ´ phase **[61].**
γ´´-strengthened alloys possess high tensile strength and good creep-rupture properties at lower temperature. After a transformation from γ´´ in γ´ at temperatures about 675° C a significant reduction in strength exists.
The crystal structure of γ" is based on a body-centred tetragonal lattice with an ordered arrangement of nickel and niobium atoms. The lattice parameters of γ" are approximately a=0.362 nm and c=0.741 nm.

8.5 Strength at high temperatures
As known the strength for most metals decreases while the temperature is increasing because the thermal activation enables the dislocations to overcome the barriers. In the opposite γ´ strengthened nickel based superalloys have a completely different behaviour because the γ´ phase is very resistant to temperature.

Slipping in γ and γ' occurs normally on the {111}<110> planes. If slipping takes place only on these planes at all temperatures then the strength would decrease with raising temperature. In the γ' phase the dislocations want to cross-slip on to the {010} planes because of their lower anti phase boundary (APB) energy there. The anti phase boundary energy decreases with temperature. There are situations in which the dislocation is on one side part of the close-packed plane and on the other side part of the cube plane **[59].**

The strength is increased when the dislocation becomes enclosed, Error! Reference source not found.. Strength decreases above 600 °C because the higher thermal activation allows the dislocations to overcome the obstacles easier, shown in Error! Reference source not found..

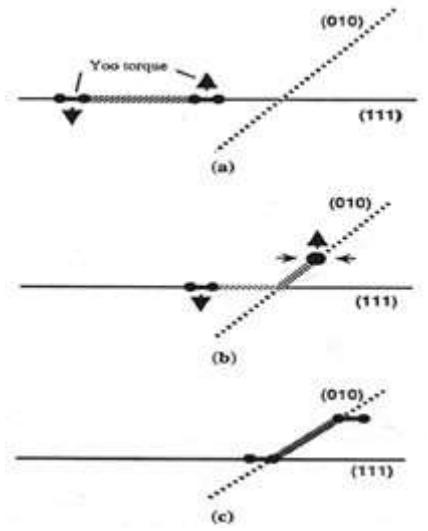

Figure 19 Cross slipping of dislocations.

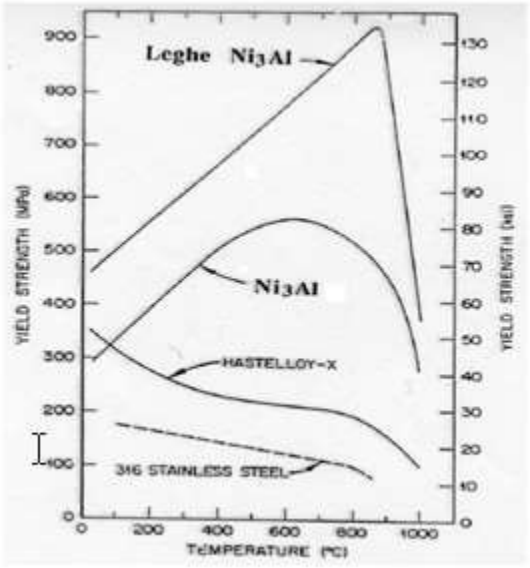

Figure 20 Strength vs temperature.

To sum up the γ` phase has the main responsibility for the excellent strength properties at high temperatures.

Behaviour of dislocations

The γ´ phase confines the movement of dislocation even though it is almost completely coherent with the γ matrix because it has an ordered crystal structure. In theγ phase the Burgers vector of a dislocation is a/2 < 100>. If that vector slips the original crystal structure does not changed as shown in **Fig. 21**. For the γ´ phase the lattice vector is a <110> like for a primitive cubic lattices. If a dislocation from the γwith the Burgers vector a/2 < 100> moves into the γ´, the order is deranged and an anti phase boundary is created. The order is restored if a slipping of a second dislocation through γ´ occurs on the same slip plane, as shown in **Fig. 22.**

As a result the penetration of γ´ has to come about by pairs of γ dislocations, called super-dislocations. This pairing process aggravates the γ dislocations to move into the γ´ phase. Therefore the creep resistance is improved.

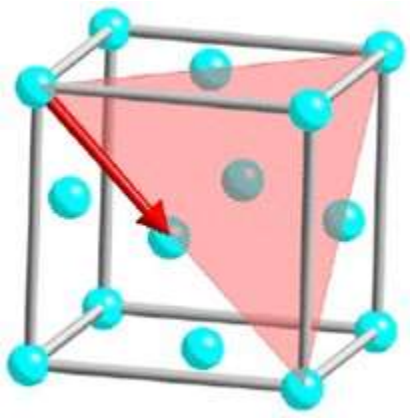

Figure 21 Dislocations in the γ phase.

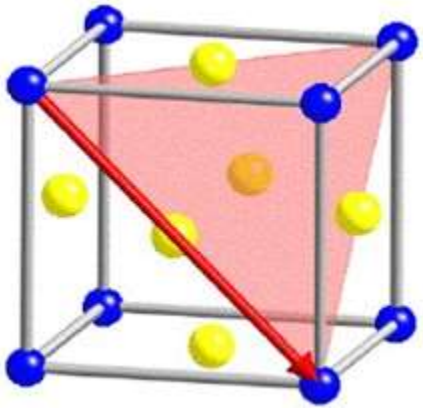

Figure 22 Dislocations in the γ´ phase.

The Burgers vectors along the <110> directions in γand γ´ are situated on {111} planes. The γ phase with the random distribution of Ni, Al, and Ti is shown in the left figure, while in the right figure the γ´ phase with the nickel atoms at the face centres is illustrated.

a) Solid solution strengthening (Mo and W).
b) Addition of elements, e.g., Co which decrease the solubility of others to promote precipitates of intermetallics.
c) Al and Ti to form ordered FCC intermetallic precipitates of gamma phase [Ni_3Al], [Ni_3Ti] **[62-66].**
d) Carbides on grain boundaries (pin boundaries to stop shear) i.e. control grain boundary sliding.
e) Small additions of B and Zr which segregate to the grain boundaries and retard sliding process and grain boundary diffusional process.
f) Large grains; columnar grains; single crystal – to stop grain boundary shear **[67].**

HEAT TREATMENT IN NI BASE SUPERALLOYS

Nickel and nickel alloys may be subjected to one or more of five principal types of heat treatment, depending on chemical composition, fabrication requirements and intended service. These methods include **[68, 69]:**

9.1. Stress Relieving

Relieving is only applied to reduce residual stresses in not precipitation strengthened materials. Time and temperature depends on the metallurgical characteristics and on the amount of residual stresses. The temperatures are normally below the annealing or recrystallization temperature.

Cast superalloys should be stress relieved if they have a complex shape (possibility of crack initiation), stringent tolerances and after they have been welded **[69].**

9.2. Annealing

Annealing is used to achieve a complete recrystallized structure with a maximum of softness, to improve ductility, to reduce hardness, to simplify forming, to prepare for welding, to reduce residual stresses and to generate specific microstructures.

This process is normally applied to wrought solid-solution-strengthened nickel based superalloys. The wrought alloys are very crack-sensitive and therefore they have to be annealed during fabrication to reduce forming and welding stresses. After annealing the grain size of the alloys depends on the amount of the prior cold or hot deformations and on the annealing temperature **[70].**

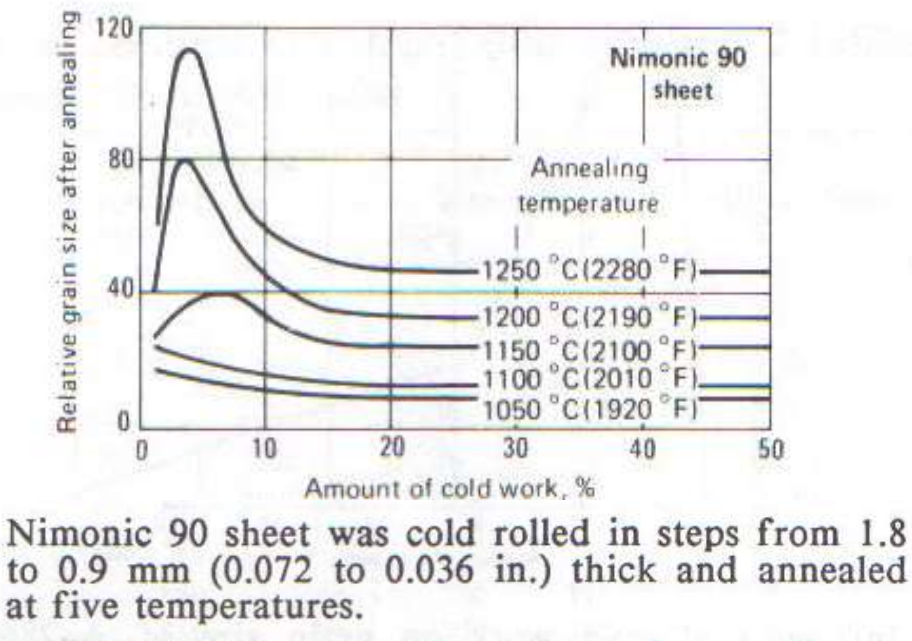

Figure 23 Effect of cold work and annealing on grain size.

The effect of cold work and annealing temperature is shown in **Figure 23.** The grain size rises with increasing annealing temperature. Above a critical amount of cold work the grain size is constant.

In general the holding time at annealing temperature amounts to 1 to 2 hours. High alloyed materials such as Astelroy require longer holding times for dissolving microconstituents.

HEAT TREATMENT FOR STRENGTHENING

10.1. Solution treating

Solution treatment is utilized to dissolve second phases to improve corrosion resistance, to prepare for following aging treatments and to homogenize the microstructure. The main task is to dissolve the γ´ phase as well as the carbides. The solution treatment temperatures of the γ´ strengthened superalloys are defined mainly by the desired properties after the aging process. The atmosphere has to be protective or even vacuum is essential.

To achieve better creep-rupture properties wrought alloys have to be heat treated at elevated temperatures. Optimum short-time tensile properties are produced at lower heat treatment temperature **[71].**

With increasing temperature an elevated grain growth exists and more carbides are dissolved. Because of this overaging the strength decreases, Error! Reference source not found.**24**. Moreover the coarser γ´ particles are the reason for lower creep-rupture strength, as shown in Error! Reference source not found..

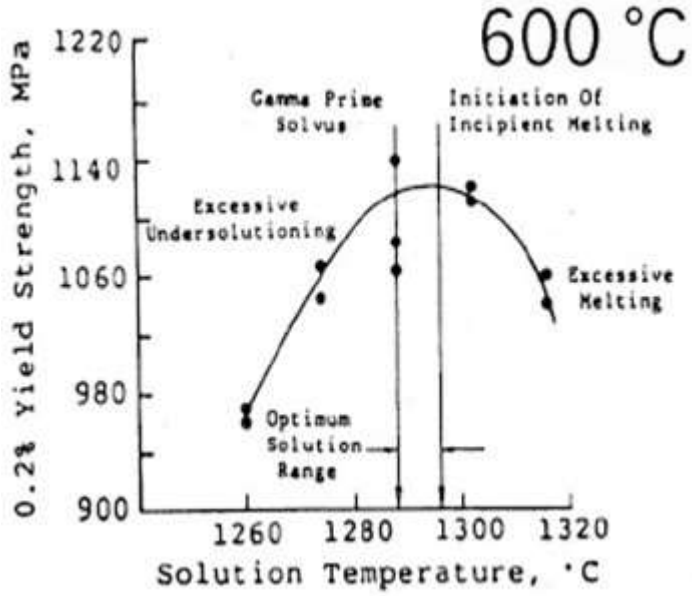

Figure 24 Yield strength vs temperature.

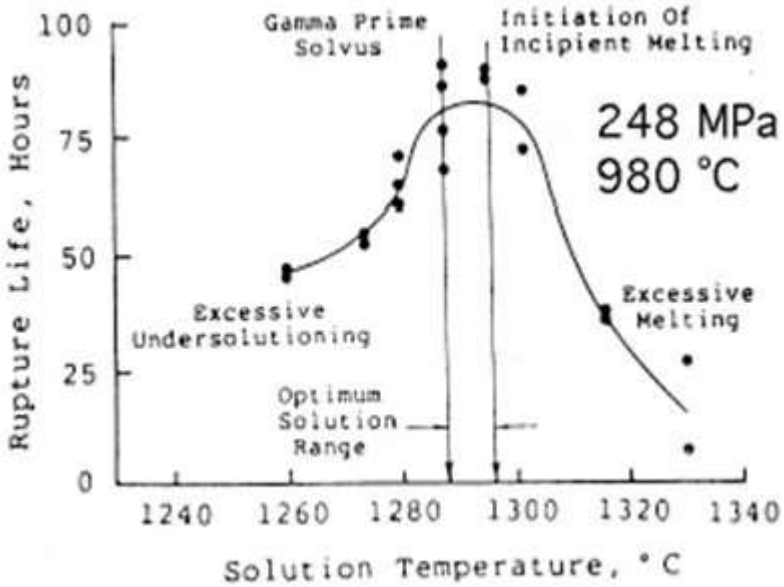

Figure 25 Creep-rupture vs solution temperature.

The diagrams illustrate that this optimal solution temperature is existent to achieve high yield strength and lengthened rupture life, Error! Reference source not found. and Error! Reference source not found..

10.2. Quenching

Quenching is used to obtain the solid-solution matrix at room temperature. Moreover it is realized to obtain a finer γ' particle size after the aging process.

10.3. Aging

Aging treatments strengthen the nickel based superalloys by precipitation of one or more phases from the supersaturated solid-solution matrix, which is generated by solution treating and retained because of quenching. The

treatment conditions depend on the type and number of precipitating phases, their size, the service temperature and on the desired mechanical properties.

The precipitated phases in nickel base superalloys can be the following **[72-74]:**

- □′-phase ($Ni_3(Al,Ti)$)
- γ" Ni_3Nb
- carbides ($M_{23}C_6$, M_6C)
- Topologically closed packed phases

The aging temperature and time determine the size distribution and forms of the precipitates.

After the aging treatment the microstructure consists of large grains which contain the main strengthening phases and a high concentration of carbides at the grain boundaries.

A treatment performed at intermediate temperatures (425 to 870ºC) on certain alloys in order to develop maximum strength by precipitation of a dispersed phase throughout the matrix. To optimize properties (often of a coating--metal system), nickel based superalloys are, after solution treatment, heat treated at two different temperatures within the γ/γ' phase field. The higher temperature heat treatment precipitates coarser particles of γ'. The second lower temperature heat treatment leads to further precipitation, as expected from the phase diagram. This latter precipitation leads to a finer, secondary dispersion of γ'. The net result is a bimodal distribution of γ', as illustrated in **Fig 26**.

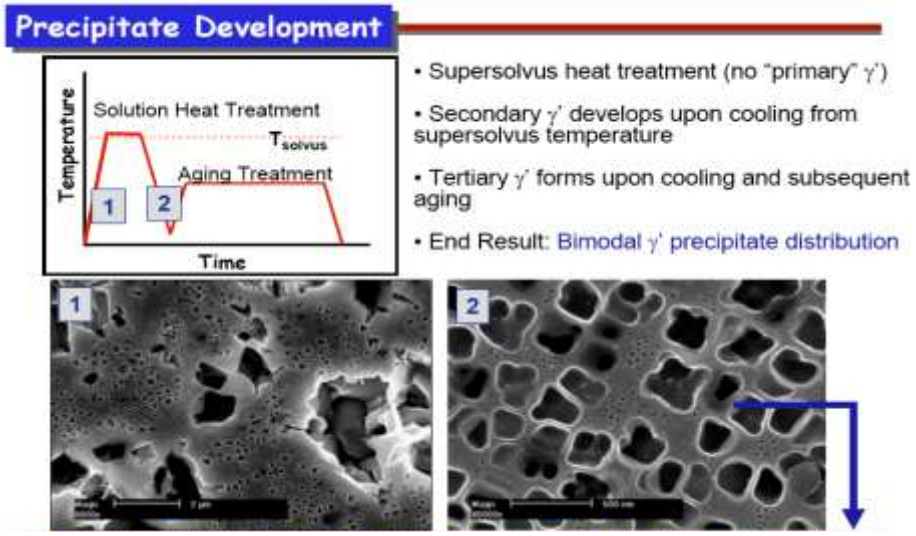

Fig. 26 The heating cycle of solution and aging and the precipitates of γ'.

PROPERTIES OF NI BASE SUPERALLOYS

Creep rupture strength

It is well indicated in that the creep-rupture-life/ gamma-prime-fraction plots are different for each series of alloys but every series is likely to have a maximum in the vicinity or more than 75 vol%. This means that the creep rupture life depends partly on solid solution hardening and partly on gamma-prime precipitation hardening. The maximum solid solution hardening is to be achieved when Cr in gamma-prime is substituted by W and Ta. Additionally gamma-prime fraction is to be obtained for the maximum precipitation hardening. In some Ni base superalloys, gamma-prime fraction in actual alloys at 1000 ºC may be smaller than that designed **[75].**

Tensile properties

Tensile properties at 900 ºC were observed for the specimen solution treated in various conditions followed by an aging treatment. Obviously the variations are well approximated with linear functions of gamma-prime fraction. Results obtained from other series of alloys have indicated that the linearities holds in the range of 50 to 80 vol% of gamma-prime fraction, which differ from the case of creep rupture strength. Effect of solution temperature is linear as well. A

higher solution temperature gives a higher yield strength. The lower the solution temperature is, the larger is the tensile elongation, but this tendency ceases to work below a certain temperature; solution treatment below 1080 ºC gave no advantage effect on tensile elongation. For the effects of solid solution hardening and precipitation hardening, clearly W is the most effective in solid solution hardening, while Ta, which is a gamma-prime former is less effective than W as a solid solution hardening element **[76].**

Hot corrosion resistance

Hot corrosion resistance was evaluated by crucible test , keeping a piece of alloy (6-8 mm in diameter and 3-5 mm in height) in a salt mixture (Na_2SO_4-25%NaCl) open to air at 900 ºC for 20h. The resistance was quantitatively specified by metal loss after all the scales being removed. Morphologically the hot corrosion was classified into three types; Type I: corrosion layer composed of Cr sulfide, Ni sulfide, and porous oxide, TypeII: corrosion layer of thin tight Cr_2O_3 with a slight or no amount of sulphide in matrix, Type III: corrosion layer composed of three layers of oxides, Cr_2O_3, TiO_2, and Al_2O_3 from outside to inside with a little amount of Cr rich sulphide dispersed in matrix. A regression analysis was carried out over 42 alloys giving type I corrosion. The results shown that Hf doped and a high Cr and Ti containing alloy, which is the most preferable in gamma-prime precipitation hardening alloys, while the addition of W, Ta, or Mo, which are essential for increase of high temperature strength, is extremely harmful for the hot corrosion **[77-79].**

COATING

The conflicting requirements of high temperature strength and corrosion resistance cannot be optimized separately in nickel based superalloys. The highest strength superalloys have been achieved through reduction of chromium with a consequent decline in corrosion resistance. Therefore it is necessary to protect the base material by an application of various coatings **[80-83].**

It can be distinguished between an oxidation resistant coating (Bond coat) and a thermal barrier coating (TBC), as shown in **Fig. 27.**

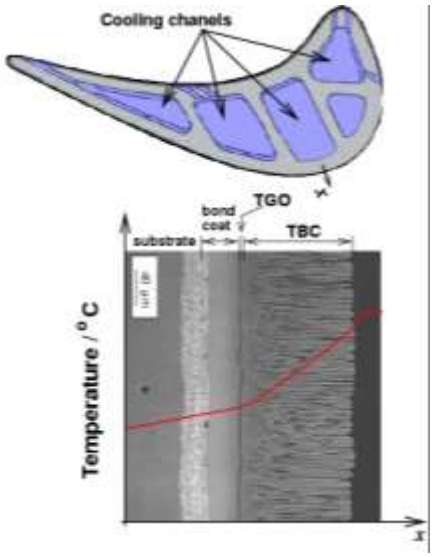

Figure 27 Cooling system and temperature profile of blades.

In this illustration the coating system in a high pressure turbine blade with the cooling system and the temperature profile is shown. The temperature declines rapidly in the TBC zone but this coating does not provide any oxidation resistance.

The two most extensive used types of bond coatings are aluminides (NiAl or Ni_2Al_3) and MCrAlY coatings. They can be produced through diffusion or coating processes such as Physical Vapour Deposition. This bond coat delivers the oxidation resistance and serves also as a transition layer between the TBC and the substrate because they have variable coefficients of expansion **[84, 85].**

APPLICATIONS OF NI BASE SUPERALLOYS

13.1 The Gas Turbine

The following Figure **(**Error! Reference source not found.**)** shows the different stages in a jet engine: intermediate pressure compressor (IPC), high pressure compressor (HPC), high pressure turbine (HPT), intermediate pressure turbine (IPT), low pressure turbine (LPT), and the pressure and temperature profiles along the engine.

It is illustrated that the conditions of temperature and pressure in the gas turbine vary strongly. Therefore different materials are used for different elements **[86].**

The red parts are fabricated of nickel based superalloys because there the highest temperatures can be found. The blue parts are produced of titanium while the orange parts of the stator are made of steel, see Fig. 29.

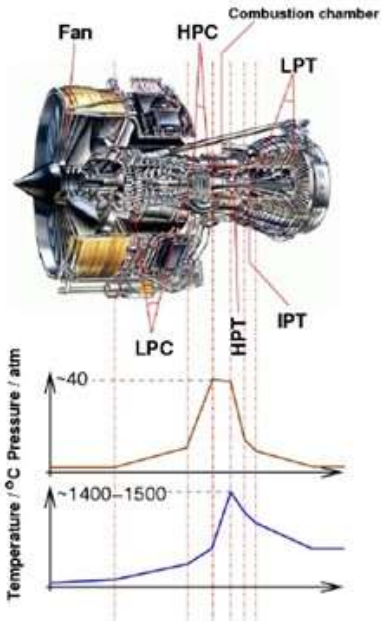

Figure 28 Temperature and pressure profile of Gas turbines.

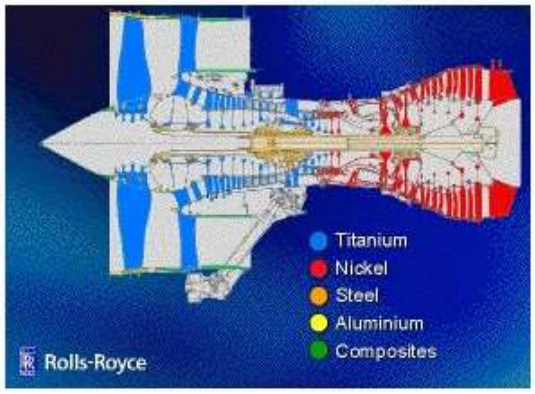

Figure 29 Materials of the Gas turbine.

The most aggressive conditions are located in the high pressure turbine with temperatures until 1400 °C and high stresses caused by rotations at more than 10000 rpm. After that the temperature decreases because the blades are cooled through a cooling system. In addition the coating system lowers also the temperature.

Coatings are widely used to improve the oxidation and hot corrosion resistance of parts of the blades.
Oxidation is defined as reaction between the coating or the base alloy with oxidants which are present in the hot gases. On the other hand hot corrosion takes place because of surface reactions with salts which were deposited from the vapour phase.

The newest turbine blades are made of single-crystal (SX). There exist no grain boundaries which function as diffusion paths. Therefore the creep resistance is improved. Another possibility to produce blades is the directional solidifying (DS). The structure exists of columnar grains but the boundaries are mostly parallel to the major stress axis. The performance of these blades is not as good as the single-crystal blades but much better than the conventionally produced equiaxed polycrystalline blades.

Steam and gas turbine blades and nozzle guide vanes, **Fig. 30** are exposed to very demanding conditions. Some of the most advanced materials and processes have been developed for such applications, which are now a major outlet for vacuum investment cast nickel-base superalloys. Complex coring technology to promote internal cooling is used routinely and effectively in blade applications. The metallurgical achievements of the directional solidification and single crystal techniques are used cost effectively in volume production, but most precision-cast airfoil components downstream of the highest temperature/pressure stages are still based on equiaxed castings **[87].**

Recently, demand has been growing for investment cast blades and fans to be used in land based turbines for power generation. Components are larger and operate at lower temperatures, but the growing demand parallels that for aero engine parts in the 1980s. This sector of the market has in fact sustained airfoil investment casters over the past few years when aircraft demand dropped.

In different fields altogether, there are a long established market for investment castings such as turbocharger, medical implants, made from stainless steel titanium and cobalt-base superalloys as shown in **Fig. 31**. **Table 5** shows the typical chemical composition of typical superalloys for vanes and turbine blades.

Nowadays Ni base superalloy IN738LC, GTD111 and MGA1400 are widely used for high temperature applications, especially for blades in recent advanced gas turbines **[87, 88],** due to its good mechanical properties at elevated temperatures, as the first stage in gas turbine.

Fig. 30 Turbine (a) Blades and (b) Nozzle guide vanes show the internal cooling channels.

Fig. 31 Different castings of superalloys produced by investment casting.

Table 5 Some alloys for vanes and blades in different turbine models of famous companies.

OEM	Model	Vanes	Blades	Coatings
Alstom (ABB)	11N2	IN939	IN738LC	NiCrAlY+Si (some rows)
	GT24/GT26	DS CM247LC(R1)/MarM247LC(R2&3)/ IN738) (R4&5)	DS CM247LC(R1-3)/MarM247LC (R4&5)	TBC (R1V)/NiCrAlY+Si (R2-4 B&V) Uncoated (R5V), Chromized (R5B)
GE	7/9EA	FSX-414 (All Stages)	GTD111(R1)/IN738(R2)/U-500(R3)	RT22 →GT29-In+ (R1B)
	7/9FA	FSX-414 (R1)/GTD222 (R2&3)	DS GTD111 (R1)/GTD111 (R2&3)	GT33-In(R1)/GT29-In+(R2)/ Chromized (R3)
	7H	SC Rene N5 (R1)/DS GTD222 (R2) Rene108 (R3)/GTD222 (R4)	SC Rene N5 (R1)/DS GTD111 (R2) DS GTD444 (R3&4) (DS version of Rene N4)	TBC (R1&2 B&V) All others GT 33
Siemens	V84/94.2	IN939 (All 4 rows)	IN738LC (R 1, 2, &3)/IN792 (R4)	CoNiCrAlY+Si (some rows)
	V84/94.3A	(SC)PWA1483 (R1&2)/IN939 (R3&4)	(SC)PWA1483 (R1&2)	TBC (EB-PVD) (R1B)/MCrAlY+Re
S-W	501D5/D5A	ECY-768 (R1&3)/X-45 (R2&4)	IN738 (R1)/U-520 (R2, 3, &4)	TBC (partial on R1V)/MCrAlY (some blade rows)
	501F	ECY-768 (R1, 2, & 3)/X-45 (R4)	IN738LC (Four rows)	TBC (R1 B&V)/MCrAlY (R2&3B)/ Sermalloy J (R4B)*
	501G	IN939 (Four rows)	DS MM002 (R1&2)/EA CM247 (R3&4) Or DS CM 247 (R1&2)	TBC (EB-PVD) (R1 B&V) TBC (R2 B&V) MCrAlY (R3 B&V)
MHI	501/701F	MGA2400 (CC Ni alloy) (Four rows)	MGA1400 CC (Similar to IN792) (Four rows)	TBC (R1 B&V)/MCrAlY (R2&3B)
	501/701G	MGA2400 (CC Ni alloy) (Four rows)	MGA1400 DS (R1&2)/MGA1400 CC (R3&4)	TBC (R1&2 B&V)/MCrAlY (R3 B&V)

GAS TURBINE BLADE CASTING

Gas turbine blades have to resist severe conditions such as elevated temperatures, high centrifugal forces and oxidation.

Nowadays directional solidification (DS) and single crystal (SX) methods are used to cast the blades because conventional casting methods create superalloys with unsatisfying high-temperature properties caused by the equiaxed grain structure.

Conventionally casted superalloys failed at the grain boundaries because of thermal fatigue, oxidation and creep. Grain boundaries are places for failure initiation. The alignment or elimination of these improves creep strength and ductility at high temperatures.

To cast turbine blades is very complicated. Simplified, a mould is made by pouring a ceramic around a wax model of the blade. Then the wax model is removed and the mould is filled with the molten metal.

Directional solidification (DS)

The directional solidification of superalloys was introduced in the sixties.

The grain boundaries are aligned parallel to the solidification direction which coincides with the principal stress axis of the component. A final structure is produced which consist of columnar grains with <001> orientation in the direction of the afterwards applied load.

DS turbine blades with the low modulus <001> orientation parallel to the direction of the applied load increase the thermal fatigue resistance drastically compared to conventionally cast turbine blades.

Single crystal (SX) casting

The process is shown in **Figure 32**. Single crystal casting is executed in vacuum in a preheated, ceramic mould.

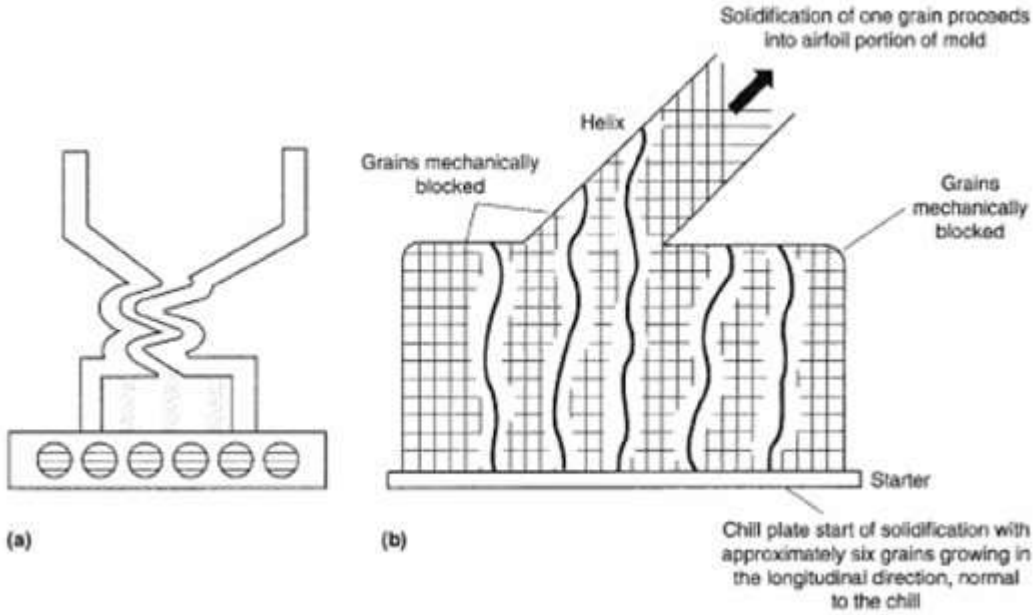

Figure 32 Single crystal processing.

Because of the controlling of the solidification in the mould, the growth of all grains can be inhibited and therefore grain boundaries are eliminated.

The mould is solidified from the bottom. At the beginning of the solidification the grains have a columnar structure which is perpendicular to the thermal gradient.

When the helical channel is reached all columnar grains except one are prevented from growing.
At the end of the helix a single crystal is produced.

Single crystal superalloys possess better high-temperature properties than DS superalloys because of the fault of grain boundary strengthening solutes such as boron and zirconium.

The missing of these elements increases the incipient melting temperature of the superalloy and thus the high-temperature properties are improved.

Moreover the alloys can be heat treated at higher temperatures in the range of 1240–1330° C. This higher heat treatment temperature allows a dissolving of all γ' and finer precipitates after the aging treatment.

In Aerospace

One of the most prevailing components in the aerospace equipment that used investment casting process to produce superalloy castings is used in Jet engines. Fig. 33 (a) and (b) shows the layout of the Jet engine, which consists of compressor, shaft, combustion chamber, turbine and exhaust nozzle. The distribution of pressure and temperature inside the Jet engine is shown in Fig. 34. The temperature level reaches the maximum in the combustion chamber. Due to the distribution of temperature and pressure in Jet engine; Fig. 29 shows the alloys and the location of these alloys in the jet engine. It is noticed that Ni base superalloys are positioned just behind the combustion chamber in Rolls Royce jet engine [89].

As seen in Fig. 35, temperature and the strength of different alloys have an inverse relationship. In the previous figure, Ti alloys have the highest strength among other alloys at lower temperatures. However, as the temperature increases the strength of Ti alloys decreases dramatically, while Ni alloys show the best strength at higher temperatures in comparison with other alloys.

In Table 5 there are some Ni base superalloys, used as Jet engine parts like blades and wheels also as rocket parts.

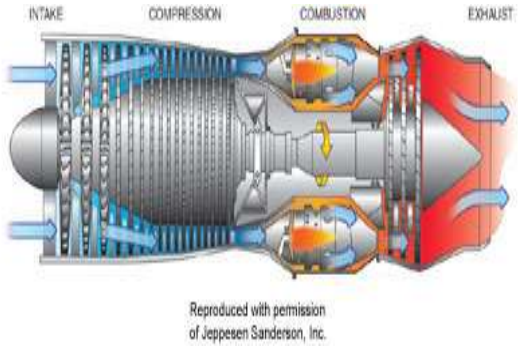

Fig. 33 a Military turbine engine.

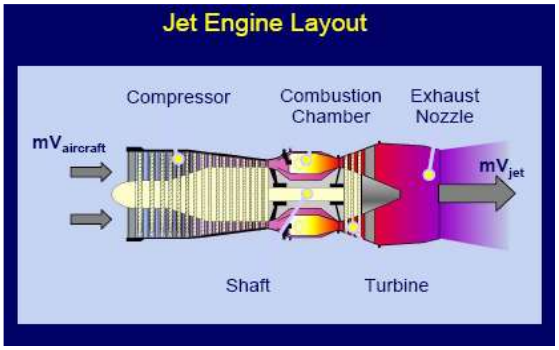

Fig. 33 b The layout of the Jet engine.

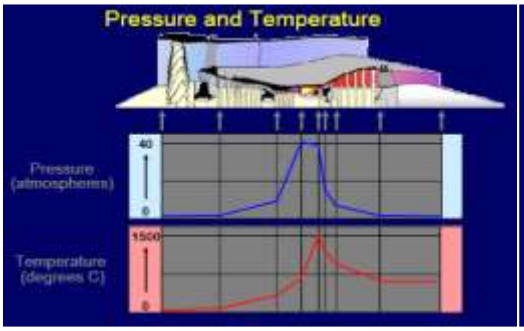

Fig. 34 Pressure and temperature distribution.

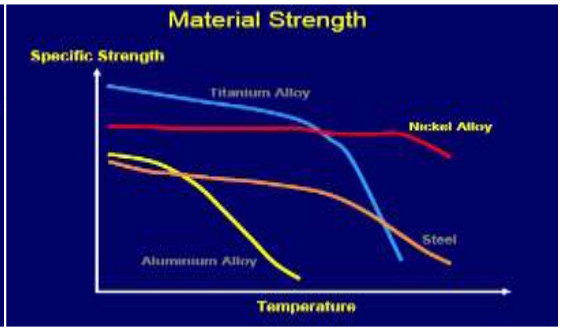

Fig. 35 Specific strength of variant alloys versus temperature.

Turbine Discs

The blades are fixed to a disc which is connected to the turbine shaft. The working temperature is much lower as the temperature of the blades. The blades must have a very good fatigue resistance.

As material can be used polycrystalline materials because the turbine discs do not have to have a resistance against creep deformation. Discs normally are produced by casting and then forged into shape. But casted discs contain some segregation which decrease the fatigue resistance. To improve fatigue resistance the recent discs are made with powder metallurgical processes, displayed in Figure 36.

Figure 36 Turbine disk.

Turbochargers

A material which is used for turbochargers can be Inconel 713C, Ni-2Nb-12.5Cr-4.2Mo-0.8Ti-6.1Al-0.12C-0.012B-0.1Zr (in wt %).

Investment Casting process is applied to produce special Nickel-based superalloy castings that are used in load-bearing structures to the highest homologous temperature of any common alloy system (T_m = 0.9, or 90% of their melting point). Among the most demanding applications for a structural material are those in the hot sections of turbine engines. The preeminence of superalloys is reflected in the fact that they currently comprise over 50% of the weight of advanced aircraft engines. The widespread use of superalloys in turbine engines coupled with the fact that the thermodynamic efficiency of turbine engines is increased with increasing turbine inlet temperatures has, in part, provided the motivation for increasing the maximum-use temperature of super alloys **[90].**

The turbocharger, shown in **Fig. 37**, supports the transportation of additional air into the engine. Consequently a larger quantity of fuel, which is burned, can be used. The device contains a turbine which works with exhaust gases from the engine. Up to 150000 rotations per minute are possible. Because of the exhaust gases the temperatures are very high and the conditions for oxidation are excellent. Therefore the material for turbochargers must have a high fatigue resistance as well as a superb resistance against oxidation.

Figure 37 Turbocharger

INFLUENCE OF CASTING FACTORS ON

14.1. Microstructure

It is widely believed that there is a need for a better correlation between casting and microstructure of Ni-superalloys **[91-93].**

Generally, the microstructure and properties of investment castings are influenced by the following parameters:

1. Superheat of liquid metal.
2. Pouring temperature
3. Shell mold temperature
4. Metal-mold-equilibrium (MME) temperature
5. Time taken to reach MME point
6. Cooling rate during solidification

The main findings of the effect of the casting processing variables on microstructural features may be concluded in the following **[94]:**

Grain Size

As all the casting properties are influenced by the grain size, selection of the optimum processing variables, based on these considerations, seems to be essential.

For Ni-base superalloys IN-100, the grain size was shown to increase with pouring temperature and/or mold temperature, with the effect of pouring temperature more pronounced. The coarser grains are promoted in thicker sections as well as at increased vacuum level, whereas the effect of the number of coats is negligible **[95].**

For investment cast IN713LC superalloy, low mold preheat temperature exhibits better controllability on grain size over the variation of pouring temperature, whereas, contrary to grain size control, high mold preheat temperature leads to better controllability of grain uniformity **[96].**

The effect of pouring temperature and superheat time on grain size is shown in **Fig. 38.** As the superheat time is increased the grain size increases as well as the increase in pouring temperature. The grain size was found to be slightly affected by the variation of inoculant content ($CoO.Al_2O_3$) **[96, 97]. Figures 39 and 40** illustrate the effect of Grain size on the properties of Ni base superalloy castings.

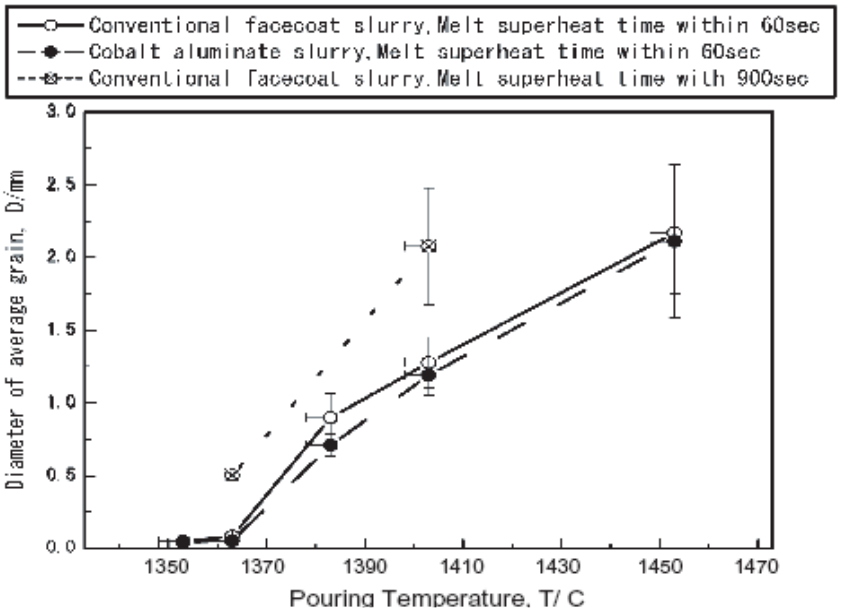

Fig. 38 Effect of Pouring temp and superheat time and $CoO.Al_2O_3$ inoculant on grain size.

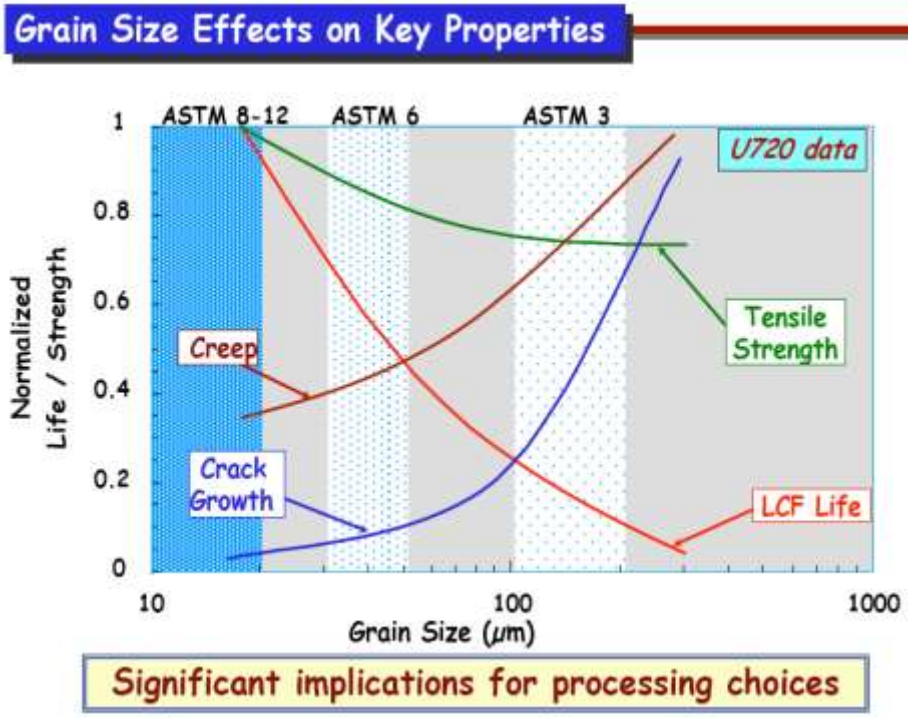

Fig. 39 The effect of garin size on properties of Ni base superalloy castings.

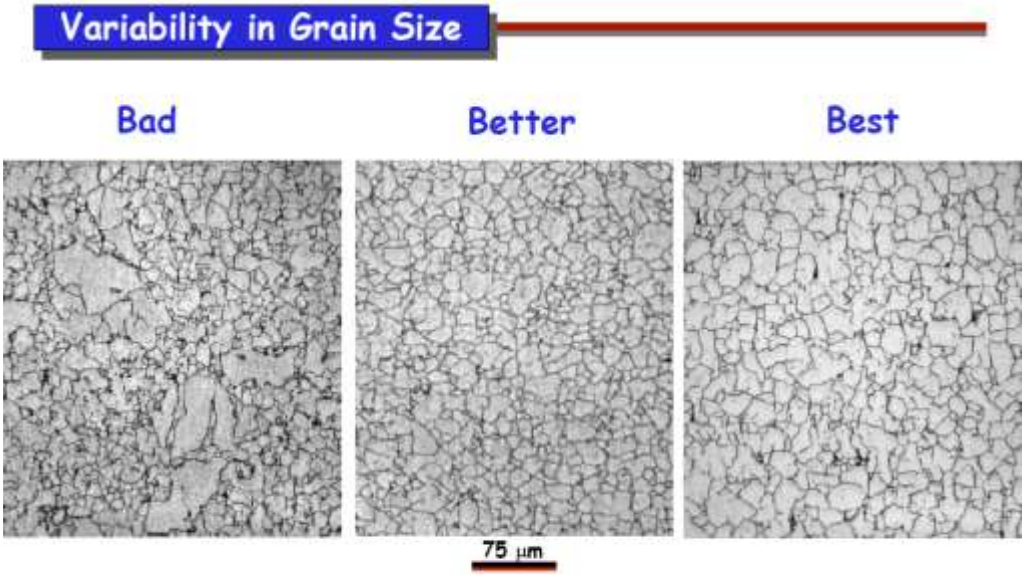

Fig. 40 Grain size distribution in Ni base superalloy castings.

Microporosity and Dendrite Arm Spacing (DAS)

Variations in DAS of IN-100 follow a trend similar to that of grain size, with the mold temperature playing a more prominent role in determining the DAS than the pouring temperature and the level of vacuum. The influence of the number of shell coats on DAS is negligible [98].

Microporosity of investment cast turbine blade of IN-713LC superalloy decreases with decreasing secondary dendrite arm spacing (SDAS). Inoculant was shown to exert some effect on decreasing the porosity content, particularly at

high mold temperatures. Porosity exists at grain boundary and interdendritic regions. Since SDAS is much finer than the grain size, the porosity content was considered to be rather a "weighing average" measure of SDAS than grain size [99]. Mold temperature exerts major effect on the porosity content because mold

temperature affects the cooling rate of casting and therefore its SDAS. When the mold temperature is high and SDAS relatively large, refinement of grain size reduces the "effective" SDAS and therefore reducing the porosity content. SDAS affect the properties of Ni base superalloy castings as shown in **Fig. 41**.

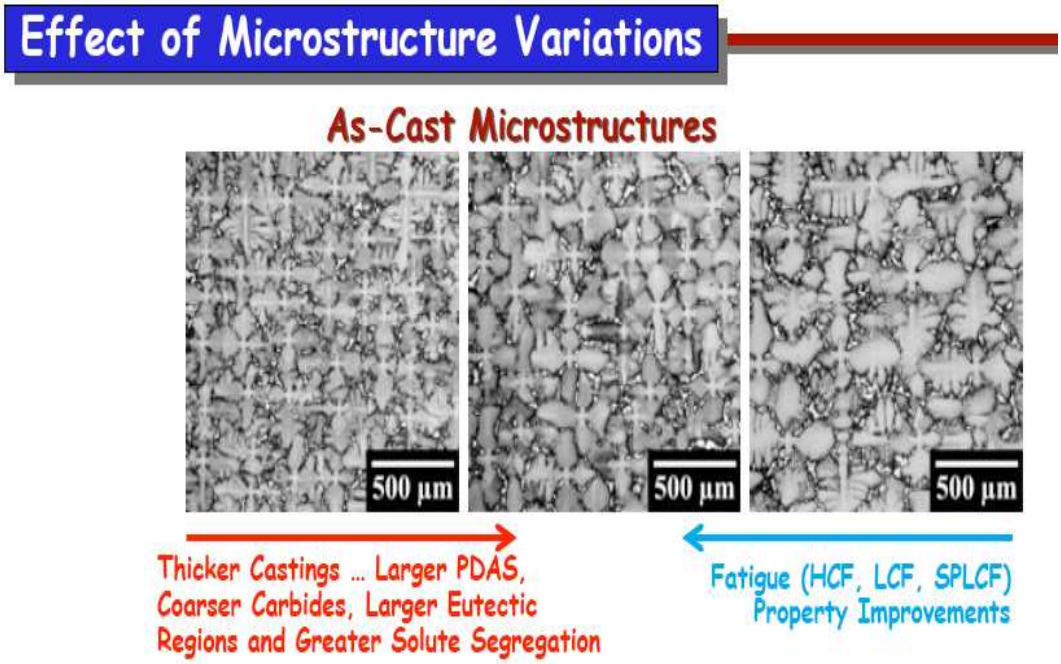

Fig. 41 Effect of SDAS on properties of Ni base superalloy castings.

Secondary Gamma Prime

Increased heat inputs, in terms of higher pouring temperature and mold temperature, result in reduced particle size of secondary gamma prime. The level of vacuum and the number of shell coats affect the morphology of the secondary gamma prime to a lesser extent **[100].** The morphology of the secondary gamma prime controls the elevated temperature properties of Ni-base superalloys and, therefore, the knowledge of the effect of the processing variables on the morphology the secondary gamma prime seems to be quite important.

Fluidity

While adequate literature is available pertaining the effect of various alloying elements on the structure and mechanical properties of investment cast Ni-base superalloys, there is hardly any information on fluidity, which is one of the most important casting characteristics of Ni-base superalloys cast in investment shells.

Woulds and Benson **[101]** reported that Ni-base superalloys high pouring temperature (1550°C), as compared to mold preheating temperature (1100°C), generates additional heat and instantaneous out-gas that becomes trapped in the mold and creates "no-fill" areas.

Brezina and Kondic **[102]** noticed that increased investment shell coatings reduced permeability of the mold wall, promoted chemical reaction of molten metal with entrapped air and consequently increased the surface tension and reduced fluidity. Vacuum was found to assist fluidity of the Ni-base superalloys either by reducing the back pressure inside the mold and/or elimination the reaction of oxygen with reactive elements in the alloy composition and thus reducing the surface tension of the molten alloy **[103]**.

Fluidity of PK24 (IN-100) alloy has been found to be quite satisfactory. Individual processing variables do affect the fluidity, but the combined effect of two or more variables on fluidity is much more pronounced. Although all the foundry variables exert influence on fluidity, the maximum effect is imposed by pouring temperature and mold temperature. Realizing satisfactory fluidity through judicious combinations of the processing variables has been proved to be a distinct possibility **[103].**

NEW TRENDS

14.2. In investment casting

Rapid prototyping

Traditionally, investment casting has been the manufacturing process of choice for certain types of castings. Ignoring for the moment those applications where investment casting is used to obtain specific material properties, users choose investment casting as a manufacturing process primarily based on two variables.

The first variable is the complexity of the geometry. For purposes of this discussion, we can define geometric complexity as features which increase the difficulty of manufacture such as undercuts, thin walls, increased accuracy, etc., Investment casting is chosen when the geometry of the casting is more complex than can be easily created by other casting methods such as sand casting, die casting or permanent mold casting. If a casting would require multiple cores to be sand cast or multiple tool actions to be die cast, then investment casting is considered.

The second variable is production volume. If the volume is too low, the amortized cost of wax pattern tooling will likely make the casting more expensive than a machined part or weldments. Investment casting is only considered when the volume is high enough that the cost of casting drops below the most of machined parts or weldments **[104, 105].**

Rapid prototyping technologies:

1- Stereo Lithography (SLA).
2- Laminated Object Manufacturing (LOM).
3- Solid Ground Curing (SGC).
4- Fused Deposition Modeling (FDM).
5- Selective Laser Sintering (SLS).
6- Direct Metal Laser Sintering (DMLS).

Figure 42 shows that the Rapid Prototyping (RP) technology saves time, especially for complex patterns shown in

Fig. 43, through using CAD models. **Figures 44 and 45** show the silicon mold and wax prototype pattern for investment casting made by RP **[106].**

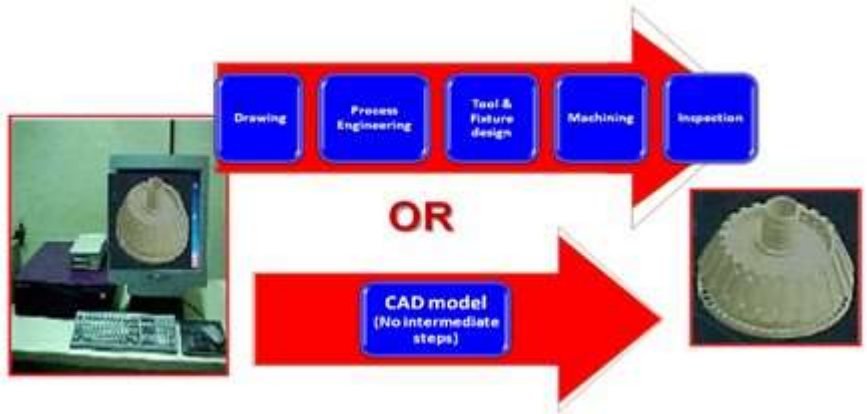

Fig. 42 Tool less additive process to convert CAD models to directly into physical parts.

Fig. 43 Complex pattern (RP). **Fig. 44 Silicon mold.** **Fig. 45 Prototype of wax pattern.**

In Ni base superalloys

Platinum base superalloys

The Platinum base superalloy development was officially started in April 1997, comprising Anglo Platinum, Impala Platinum, Lonmin (then Lonrho) and Mintek. The aim was to encourage new research into Pt-based alloys which would eventually lead to an increased use of Pt, by broadening the industrial base. It was hoped that further research would be spawned following publication of the PDI's research, and the world network of Pt researchers would grow. The major topic was identified as the development of new alloys based on Pt which would probably have similar microstructures to the Ni-based superalloys and could be used at even higher temperatures, as well as in more aggressive environments **[106-110]. Figure 46** shows the ultimate strength against temperature for both Ni and Pt base superalloys.

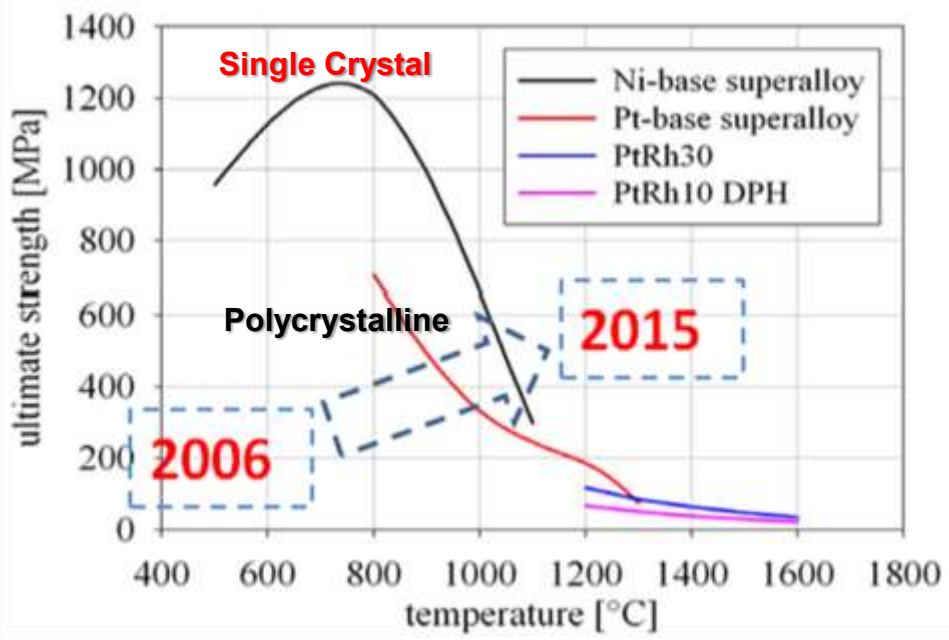

Fig. 46 Ultimate strength versus temperature for Ni and Pt base superalloys.

Is it possible to copy the microstructure from Ni to Pt?

Only Ir, 2466°C and Rh, 1964°C are fcc metals with an even higher melting point and ductile throughout the temperature range. Best corrosion and oxidation resistance amongst metals (volatile oxide, but very low oxidation rate). Pt_3Al has the same $L1_2$ structure as Ni_3Al.

Advantages

- Microstructure can be copied from (Ni + Ni_3Al) to (Pt + Pt_3Al).
- Misfit can be adjusted.

• Volume fraction can be adjusted.
• Mechanical strength in a temperature window 1250°C to 1350°C superior than any other known material with the constrictions: RT-ductility and testing in air.
• Possible application: steering rockets for satellites**.**

Disadvantage
• Price: Pt-alloy turbine blade would increase cost by a factor of 3 to 5.
• Only small parts (helicopter turbine).
• Density: ρPt-alloy ~ 20 g/cm^3, ρNi-alloy ~ 9 g/cm^3.
• Centrifugal load factor of ~ 2.2 higher. With a stress exponent n = 4.
• 24 x higher creep rate.
• Pt-alloys cannot replace moving parts in a turbine.

Nanoparticles unlock the future of superalloy metals.
'Sandia National Laboratories is pioneering the future of superalloy materials by advancing the science behind how those superalloys are made. As part of Sandia's nanoscale research, a group of experts specializing in inorganic synthesis and characterization, modeling, and radiation science have designed a radical system of experiments to study the science of creating metal and alloy nanoparticles.

This research has vast implications, says Tina Nenoff, project leader. The lightweight, corrosion-resistant materials that the team is creating are needed for weapons casings, gas turbine engines, satellites, aircraft, and power plants.

A quick trip down memory lane to the days of high school science class will recall those chapters on material and chemical science defining alloys as a combination of two or more elements, at least one of which is a metal, where the resulting material has metallic properties different- sometimes significantly different- from the properties of its components. For instance, steel is stronger than iron, its primary component **[111].**

Superalloys, as the name would imply, stand out from the general population of alloys in the same way Superman would be considered extraordinary compared to the rest of us. These specialized alloys are exceptionally strong, lightweight, and able to withstand extremes that would destroy everyday metals like steel and aluminum.

"These high-performance superalloys are revered for their remarkable mechanical strength and their resistance to corrosion, oxidation, and deformation at high temperatures," says Jason Jones, Sandia researcher.'

Beyond Ni base superalloys
In order to achieve service temperatures higher than those of nickel-base superalloys, materials with significantly higher melting points are required. In the sixties, refractory alloys based on Nb and Mo was considered, but their oxidation resistance was inadequate and no sufficiently effective protective coating systems were found. More recently, systems based on $MoSi_2$ and NiAl were considered. Although these systems, in particular $MoSi_2$, have excellent oxidation resistance, their creep strength could not be improved to match or exceed that of nickel-base superalloys. Therefore interest in $MoSi_2$ and NiAl based system has waned. Presently, attention is focused on niobium silicides, molybdenum borosilicides, **Fig. 47,** and iridium-base super alloys **[112, 113].**

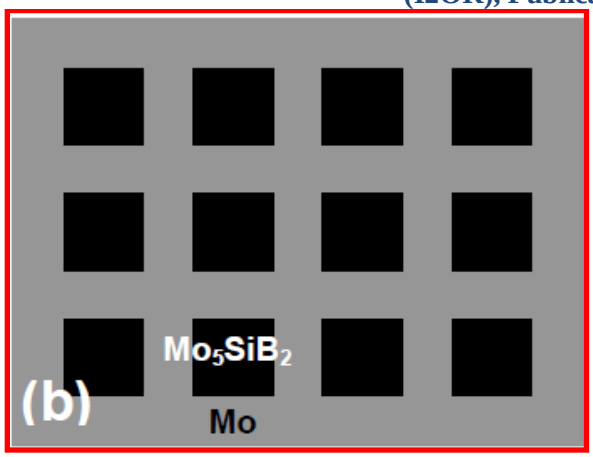

Fig. 47 Schematic illustration of Mo_5SiB_2 microstructure.

REFERENCES

[1] M. J. Donatchie Jr. and S. J. Donatchie, Superalloys: A Technical Guide, 2nd ed. (Materials Park, OH: ASM International, 2002).
[2] "Superalloys II," edited by C. T. Sims, N. S. Stoloff and W. C. Hagel (New York: John Wiley and Sons, 1987).
[3] S. Walston, A. Cetel, R. MacKay, K. O'Hara, D. Duhl and R. Dreshfield; in Superalloys 2004; edited by K. A. Green, T. M. Pollock, H. Harada, T. E. Howson, G. C. Reed, J. J. Schirra and S. Walston (Warrendale, PA, USA: TMS, 2004), 15.
[4] A. Sato, H. Harada, T. Yokokawa, T. Murakumo, Y. Koizumi, T. Kobayashi and H. Imai; " Scripta Materialia, 54 (2006) 1679.
[5] F. Pyczak, B. Devrient, F. C. Neuner and H. Mughrabi; Acta Materialia, 53 (2005), 3879.
[6] K. Durst and M. Goken; Materials Science and Engineering A, 387-389 (2004) 312.
[7] A. C. Yeh and S. Tin; Scripta Materialia, 52 (2005) 519.
[8] C. M. F. Rae and R. C. Reed; Acta Materialia, 49 (2001) 4113.
[9] F. Long, Y.S. Yoo, C.Y. Jo, S.M. Seo, Y.S. Song, T. Jin, Z.Q. Hu, Mater. Sci. Eng. A 527 (2009) 361.
[10] S.A. SAjjadi, S.M. Zebarjad, R.I.L. Guthrie, M. Isac, Mater. Process. Technol. 175 (2006) 376.
[11] Reed, R.C.: The Superalloys, Fundamentals and Applications, Cambridge University Press, New York, USA, 2006.
[12] Sims. C.T., Stoloff. N.S. and Hagel. W.C., (1987) Superalloys II- High Temperature Materials for Aerospace and Industrial Power, John Wiley & Sons Inc., USA.
[13] M. Pouranvari, A. Ekrami, A.H. Kokabi, Alloys Compd. 461(2008) 641.
[14] A. Jacques, F. Diologent, P. Caron, P. Bastie, Mater. Sci. Eng. A 483–484 (2008) 568.
[15] C.T. Sims and W.C. Hagel, The Superalloys, John Wiley and Sons Inc., Canada, 1972
[16] L.Z. He, Q. Zheng, X.F. Sun, H.R. Guan, Z.Q. Hu, A.K. Tieu, C. Lu, H.T. Zhu, Mat. Sci. Eng. A, 397 (2005) 297–304
[17] L.R. Liu, T. Jin, N.R. Zhao, X.F. Sun, H.R. Guan, Z.Q. Hu, Materials Science and Engineering A 361 (2003) 191-197.
[18] X.Z. Qin, J.T. Guo, C. Yuan, J.S. Hou, H.Q. Ye, Materials Letters, 62 (2008) 2275-2278.
[19] R.A. Kupkovits, D.J. Smith, R.W. Neu, Procedia Eng. 2 (2010) 687.
[20] M. Pouranvari, A. Ekrami, A.H. Kokabi, Mater. Sci. Eng. A 490 (2008) 229.
[21] H. Xuebing, K. Yan, Z. Huihua, Z. Yun, H. Zhuangqi, Mater. Lett. 36 (1998) 210.
[22] Z. Chu, J. Yu, X. Sun, H. Guan, Z. Hu, Mater. Sci. Eng. A 527 (2010) 3010.
[23] MJ Donachie and SJ Donachie, 'Superalloys: a technical guide', 2nd ed (2002) ASM International.
[24] R Schneider et al, Proc. 5th Int. Conf. on Tooling, Leoben, Austria (1999) 265.
[25] W.R. Sun, J.H. Lee, S.M. Seo, S.J. Choe, Z.Q. Hu, Mater. Sci. Technol. 15 (1999) 1221.
[26] B.G. Choi, I.S. Kim, D.H. Kim, C.Y. Jo, Mater. Sci. Eng. A 478 (2008) 329

[27] S.M. Seo, I.S. Kim, J.H. Lee, C.Y. Jo, H. Miyahara, K. Ogi, Metall. Mater. Trans. A 38 (2007) 883.
[28] G. Lvov, V.I. Levit, M.J. Kaufman, Metall. Mater. Trans. A, 35A (2004) 1669.
[29] X.Z. Qin, J.T. Gou, C. Yuan, C.L. Chen, H.Q. Ye, Metall. Mater. Trans. A, 38A (2007) 3014.
[30] Xiurong Guan, Enze Liu, Zhi Zheng, Yongsi Yu, Jian Tong and Yuchun Zhai, J. Mater. Sci. Technol. 27 ((2011) 113.
[31] C.M.F. Rae, R.C. Reed, Acta Mater. 49 (2001) 4113.
[32] R C Reed, `The Superalloys: Fundamentals and Applications', Cambridge University Press (2006).
[33] Nakagawa Y., Green K.A., Superalloys (2004) TMS, 3.
[34] Xiangbin Meng, Jinguo Li, Tao Jin, Xiaofeng Sun, Changbo Sun and Zhuangqi Hu, Journal of Materials Science & Technology, 27 (2) February (2011) 118.
[35] Y. Koizumi, T. Kobayashi, Z. Jianxin, T. Yokokawa, H. Harada,Y. Aoki, and M. Arai, Proceedings of the International Gas Turbine Congress 2003 Tokyo November 2-7, 2003.
[36] Caron P. and Khan T., Aerosp. Sci. Techno. 3 (1999) 513.
[37] R. Burgel, J. Grossmann, O. Luserbrink, H. Mughrabi, F. Pyczak, R. F. Singer and A. Volek; in Superalloys 2004; edited by K. A. Green, T. M. Pollock, H. Harada, T. E. Howson, G.C. Reed, J. J. Schirra and S. Walston (Champion, PA, USA: TMS (2004) 25.
[38] F. Diologent and P. Caron; Materials Science and Engineering A, 385 (2004) 245.
[39] Rolls Royce Company, Jet Engine. civil.rolls-royce.com/civil-aircraft-engine-pictures.
[40] I. Okada, T. Torigoe, K. Takahashi and D. Izutsu; in Superalloys 2004; edited by K. A. Green, T. M. Pollock, H. Harada, T. E. Howson, G. C. Reed, J. J. Schirra and S. Walston (Champion, PA, USA: TMS, 2004), 702.
[41] C. T. Sims and W. C. Hagel "The Superalloys," (New York: John Wiley and Sons, 1972).
[42] R. Hashizume, A. Yoshinari, T. Kiyono, Y. Murata and M. Morinaga; " in Superalloys 2004; edited by K. A. Green, T. M. Pollock, H. Harada, T. E. Howson, R. C. Reed, J. J. Schirra and S. Walston (Warrendale, PA: TMS (The Minerals, Metals & Materials Society), (2004) 53.
[43] T. Kobayashi, Y. Koizumi, T. Yokokawa and H. Harada; Journal of the Japan Institute of Metals, 66 (9) (2002) 897.
[44] N. El-Bagoury, K. Yamamoto, H. Miyahara and K. Ogi; Materials Transactions, 46 (2005) 909.
[45] K. Tsukagoshi and S. Shiozaki and Y. Tsukuda, Mitsubishi Heavy Industry, Japan.
[46] Sunao Aoki, Proceedings of 2000 International Joint Power Generation Conference, Miami beach, Florida, July 23-26 (2000).
[47] T.B. Gibbons, S. Osgerby, F. Gabrielli and V. Lupino: Materials Science and Technology, vol. 3, No. 4, April (1987) 268.
[48] A. Sato, Y. Koizumi, T. Kobayashi, T. Yokokawa, H. Harada and H. Imai, J. Japan Inst Metals, 68 (2004) 507–510.
[49] K. O'Hara, W.S. Walston, E.W. Ross and R. Darolia, U.S. Patent 5, 482, 789, "Nickel Base Superalloy and Article", 1996.
[50] Y. Koizumi, T. Kobayashi, T. Yokokawa, H. Harada, Y. Aoki, M. Arai, S. Masaki and K. Chikugo, "Development of 4th Generation Single Crystal Superalloys", Proceedings (2nd International Symposium on High Temperature Materials, Tsukuba, Japan, 31 May – 2 June (2001), pp. 30–31.
[51] J. X. Zhang, T. Murakumo, Y. Koizumi, T. Kobayashi, H. Harada and S. Masaki, Metall. Mater. Trans. A, 33A (2002) 3741–3746.
[52] Y. Koizumi, T. Kobayashi, T. Yokokawa, J. X. Zhang, M. Osawa, H. Harada, Y Aoki and M. Arai, "Development of Next-Generation Ni-Base Single Crystal Superalloys", Superalloys 2004, (TMS, 2004), pp. 35–43.
[53] S. Walston, A. Cetel, R. MacKay, K. O'Hara, D. Duhl and R. Dreshfield, "Joint Development of a Fourth Generation Single Crystal Superalloy", Superalloys 2004, (TMS, 2004), pp. 15–24.
[54] K. Kawagishi, A. Sato, T. Kobayashi and H. Harada, J. Japan Inst. Metals, 69 (2005) 249–252.
[55] Kyoko Kawagishi, An-Chou Yeh, Tadaharu Yokokawa, Toshiharu Kobayashi, Yutaka Koizumi and Hiroshi Harada, "DEVELOPMENT OF AN OXIDATION-RESISTANT HIGH-STRENGTH SIXTHGENERATION SINGLE-CRYSTAL SUPERALLOY TMS-238", Superalloys 2012: 12th International Symposium on Superalloys, Edited by: Eric S. Huron, Roger C. Reed, Mark C. Hardy,

Michael J. Mills, Ric E. Montero, Pedro D. Portella, Jack Telesman, TMS (The Mineral, Metals & Materials Society).
[56] L.E. Dardi, R.P. Dalal and C. Vaker: Advanced High-Temperature Alloys: Processing and Properties, Proceedings of the Nicholas J. Grant Symposium on Processing and Properties of Advanced High-Temperature Alloys (Ed. S.M. Allen et al.), ASM Metals Park Ohio (1986).
[57] F. Long, Y.S. Yoo, S.M. Se, T. Jin, Z.Q. Hu and C.Y. Jo, J. Mater. Sci. Technol., 27 (2) (2011) 101.
[58] R.F. Smart: Metallurgy and Metal Forming, 44 (7) July (1977) 286.
[59] Alexander Galge, Nickel-based superalloys and their application in the aircraft industry, Facolta di Ingegneria, Universita' Degli Studi di Trento, 2006.
[60] Tin, S., Pollock, T.M. King, W.T.: Carbon addition and grain boundary formation in high refractory nickel-based single crystal superalloys, in T.M. Pollock, R.D. Kissinger, R.R. Bowman et al., eds. Superalloys 2000, Warrendale,PA: The Minerals, Metals and Materials Society (TMS), pp. 201-210, 2000.
[61] A.K. Koul, R. Thamburaj, Metallurgical Transactions A (Physical Metallurgy and Materials Science), 16A (1985) 17-26.
[62] A.D. Sequeira, H.A. Calderon, G. Kostorz, Scripta Metallurgica Materialia 30 (1994) 75.
[63] T. Grosdidier, 55. A. Hazotte, A. Simon, Scripta Metallurgica Materialia 30 (1994) 1257.
[64] S. Kraft, I. Altenberger, H. Mughrabi, Scripta Metallurgica Materialia 32 (1995) 411.
[65] Y. Y. Qiu, Acta Materialia 44 (1996) 4969 .
[66] H.S. Chandraseckariah and S. Seshan: AFS Transactions (1995) 611.
[67] H.J. Burkhardt, Quintessenz Zahntech 31(2) (2005) 136.
[68] Nader El-Bagoury, Archives of Applied Science Research, 3 (2) (2011) 266.
[69] Watanabe I., J.Liu, N.Baba, T.Okabe, Dent Mater 20 (7) (2004) 630.
[70] I.Watanabe, A.P. Benson, K.Nguyen J Prosthodont 14 (3) (2005) 170.
[71] W. Fu, Z. Jun-tao, W. Xian-hui, F. Zhi-kang, Trans. Nonferrous Met. Soc. China 19 (2009).
[72] N. El-Bagoury, M. Waly, A. Nofal, Mater. Sci. Eng. A 487 (2008) 152.
[73] E. Balikci, A. Raman, R.A. Mirshams, Metall. Mater. Trans. A, 28A (1997) 1993.
[74] J. Plan, Acta Metallurgica Slovaca, 17 (1) (2011) 38.
[75] A. Mottura, M. W. Finnis, and R. C. Reed, Acta Materialia, 60 (2012) 2866.
[76] Metal Handbook tenth edition – Vol 1 – Properties and Selection: Iron, Steel, and High- Performance Alloys, ASM INTERNATIONAL, Materials Park, Ohio, 2005.
[77] E. Chang and J.C. Chou, "J. of Chinese Foundrymen's Association (1986) 1.
[78] H.Harada, M.Yamazaki, Y.Koizumi, N.Sakuma, N.Furuya and H.Kamiya'National Research Institute for Metals Tsukuba-city, Ibaraki, Japan, Central Research Laboratory, Daido Steel Co., Ltd. Minami-ku, Nagoya, Japan Published in Proceedings of a Conference, held in Liege, Belgium, 4-6 Oct. 1982 D.Reidel Publishing Co.
[79] H.-E. Zschau, P. J. Masset and M. Schu¨tze, Materials and Corrosion, 62 (2011) 1.
[80] D.R. Clarke, Surf. Coat. Technol., 163-164 (2003) 67-74.
[81] C.G. Levi, Mater. Sci., 8 (2004) 77-91.
[82] M. Gell, P.G. Klemens, Mat. Sci. Eng. A, 245 (1997) 143-149.
[83] Y. Shen, R.M. Leckie, C.G. Levi, D.R. Clarke, Acta Mater., 58 (2010) 4424-4431.
[84] I. Gurrappa, A.S. Rao, Surface & Coatings Technology, 201 (2006) 3016- 3029.
[85] G. W. Goward, Surface and Coatings Technology, 108-109 (1998) 73-79.
[86] T.B. Gibbons, Materials Science and Technology, 25 (2009) 129-135.
[87] R. C. Reed, J. J. Moverare, A. Sato, F. Karlsson, and M. Hasselqvist, "A new single-crystal superalloy for power generation applications," in Superalloys 2012 (E. S. Huron, R. C. Reed, M. Hardy, M. J. Mills, R. E. Montero, P. D. Portella, and J. Talesman, eds.) The Minerals, Metals and Materials Society (2012) 197.
[88] N. Das, Transactions of The Indian Institute of Metals, 63 (2010) 265-274.
[89] Enze Liuy, Zhi Zheng, Xiurong Guan, Jian Tong, Likui Ning and Yongsi Yu, J. Mater. Sci. Technol., 26 (2010) 895.
[90] Lei Z., Zhang M. and Dong J., Journal of Materials & Design 32 (2011) 1981.
[91] L. Liu, T.W. Huang, M. Qu, et al. Journal of Materials Processing Technology, 210 (2010) 159-165.

[92] Y. Zhuhuan, L. Lin, Z. Xinbo, et al. China Foundry, 7 (2010) 217-223.
[93] Z. Xinbao, L. Lin, Y. Zhuhuan, et al. Journal of Materials Science, 45 (2010) 6101-6107.
[94] J.C. Tucker, L.H. Chan, G.S. Rohrer, M. A. Groeber and A.D. Rolletta, Scripta Materialia 66 (2012) 554–557.
[95] D. Kobayashi1, A.T. Yokobori, R. Sugiura and A. Fuji, Materials Transactions, 51 (2010) 220 -2207.
[96] S.A. SAjjadi, S.M. Zebarjad, R. I. L. Guthrie, M. Isac, Materials Processing Technology, 175 (2006) 376.
[97] M. Pouranvari, A. Ekrami, A.H. Kokabi, Alloys and Compounds 461 (2008) 641.
[98] A. Jacques, F. Diologent, P. Caron, P. Bastie, Materials Science and Engineering A, 483–484 (2008) 568.
[99] N. D'Souza, H. B. Dong, M. G. Ardakani, B. A. Shollock, Scripta Materialia, 53 (2005) 729-733. M. Woulds and H. Benson: Superalloy 1984, Proceedings of the Fifth International Symposium on Superalloys, (Ed. M. Gell et al.), The Metallurgical Society of ASME, Warrendale, DA Sept. (1984) 3.
[100] M. Brezina and V. Kondic: the British Foundryman, 66, Dec. (1993) 337.
[101] J. Campbell and I.D. Olliff: AFS Cast Metals Research Journal, 7, June (1971) 55.
[102] G. CAO, S. KOU, Met. Trans. A. 37A, (2006), p.3647.
[103] Centrum Prof. Čecha s.r.o. Anatomie koleního kloubu [online]. World Wide Web: http://www.ortopedie fyzioterapie.cz/ortopedicka-ambulance/umely-kolenni-loub.html [cit. January, 20. 2009].
[104] M. Horacek, O. Charvat, V. Smrcka. Rapid wax patterns obtained by RP and silicone mould technologies. In: Proceedings of the 48th Conference Portoroz, 2009: 57.
[105] M. Horáček, O. Charvát, T. Pavelka, J. Sedlák, M. Madaj, J. Nejedlý, and J. Dvořáček, The 69th WFC February (2011) 107.
[106] L. A. Cornish, R. Süss, A. Watson and S. N. Prins, Platinum Metals Rev., 51 (2007) 104.
[107] L. A. Cornish, R. Süss, L. H. Chown, A. Douglas, M. Matema, L. Glaner and G. Williams,"International Platinum Conference 'Platinum Surges Ahead'", Sun City, South Africa, 8th–12th October, 2006, Symposium Series S45, The Southern African Institute of Mining and Metallurgy, Johannesburg, South Africa (2006) 57.
[108] N. B. Maledi, J. H. Potgieter, M. Sephton, L. A. Cornish, L. Chown and R Süss, "International Platinum Conference 'Platinum Surges Ahead", Sun City, South Africa, 8th–12th October, 2006, Symposium Series S45, The Southern African Institute of Mining and Metallurgy, Johannesburg, South Africa (2006) 81.
[109] J. Preußner, S. N. Prins, M. Wenderoth, R. Völkl and U. Glatzel, Platinum Metals Rev. 52 (2008) 48.
[110] Muktarov Sh, and Ermakhenko A., Journal of Physics: Conference Series 240 (2010) 118.
[111] J. H. Schneibel, "High temperature strength of Mo-Mo3Si-Mo5SiB2 molybdenum silicides," Intermetallics 11 (2003) 625.
[112] C. Huang, Y. Yamabe-Mitarai, S. Nakazawa, and H. Harada, Materials Letters 58 (2004) 483.